


Binding of phosphatidylserine-positive microparticles by PBMCs classifies disease severity in COVID-19 patients

Lisa Rausch¹ | Konstantin Lutz¹ | Martina Schifferer^{2,3} | Elena Winheim¹ |
 Rudi Gruber⁴ | Elina F. Oesterhaus^{5,6} | Linus Rinke¹ | Johannes C. Hellmuth^{5,7} |
 Clemens Scherer^{5,8} | Maximilian Muenchhoff^{5,6,9} | Christopher Mandel^{5,10} |
 Michael Bergwelt-Baildon^{5,7} | Mikael Simons^{2,3,11} | Tobias Straub¹² | Anne B. Krug¹ |
 Jan Kranich¹  | Thomas Brocker¹ 

¹ Institute for Immunology, Biomedical Center (BMC), Faculty of Medicine, LMU Munich, Munich, Germany

² German Center for Neurodegenerative Diseases (DZNE), Munich, Germany

³ Munich Cluster of Systems Neurology (Synergy), Munich, Germany

⁴ bene pharmaChem GmbH & Co.KG., Geretsried, Germany

⁵ COVID-19 Registry of the LMU Munich (CORKUM), University Hospital, LMU Munich, Munich, Germany

⁶ Max von Pettenkofer Institute & Gene Center, Virology, National Reference Center for Retroviruses, LMU München, Munich, Germany

⁷ Department of Medicine III, University Hospital, LMU Munich, Munich, Germany

⁸ Department of Medicine I, University Hospital, LMU Munich, Munich, Germany

⁹ German Center for Infection Research (DZIF), partner site Munich, Germany

¹⁰ Department of Medicine IV, University Hospital, LMU Munich, Munich, Germany

¹¹ Institute of Neuronal Cell Biology, Technical University of Munich, Munich, Germany

¹² Core facility Bioinformatics, Biomedical Center (BMC), Faculty of Medicine, LMU Munich, Munich, Germany

Correspondence

Prof. Dr. Thomas Brocker, Institute for Immunology, Biomedical Center (BMC), Faculty of Medicine, LMU Munich, Großhaderner Str. 9, D-82152 Planegg-Martinsried, Germany.
 Email: brocker@lmu.de

Jan Kranich and Thomas Brocker shared senior authorship.

Funding information

Deutsche Forschungsgemeinschaft (DFG, German Research Foundation), Grant/Award Numbers: Project-ID 210592381 - SFB 1054: TP B03, A06, Project-ID 369799452 - SFB/TR237: TP B14, Project-ID 391217598 - KR2199/10-1; Bavarian State Ministry of Science and the Arts

Abstract

Infection with SARS-CoV-2 is associated with thromboinflammation, involving thrombotic and inflammatory responses, in many COVID-19 patients. In addition, immune dysfunction occurs in patients characterised by T cell exhaustion and severe lymphopenia. We investigated the distribution of phosphatidylserine (PS), a marker of dying cells, activated platelets and platelet-derived microparticles (PMP), during the clinical course of COVID-19. We found an unexpectedly high amount of blood cells loaded with PS⁺ PMPs for weeks after the initial COVID-19 diagnosis. Elevated frequencies of PS⁺ PMP⁺ PBMCs correlated strongly with increasing disease severity. As a marker, PS outperformed established laboratory markers for inflammation, leucocyte composition and coagulation, currently used for COVID-19 clinical scoring. PS⁺ PMPs preferentially bound to CD8⁺ T cells with gene expression signatures of proliferating effector rather than memory T cells. As PS⁺ PMPs carried programmed death-ligand 1 (PD-L1), they may affect T cell expansion or function. Our data provide a novel marker for disease severity and show that PS, which can trigger the blood coagulation cascade, the complement system, and inflammation, resides

This is an open access article under the terms of the [Creative Commons Attribution-NonCommercial-NoDerivs License](https://creativecommons.org/licenses/by-nc-nd/4.0/), which permits use and distribution in any medium, provided the original work is properly cited, the use is non-commercial and no modifications or adaptations are made.

© 2021 The Authors. *Journal of Extracellular Vesicles* published by Wiley Periodicals, LLC on behalf of the International Society for Extracellular Vesicles

on activated immune cells. Therefore, PS may serve as a beacon to attract thromboinflammatory processes towards lymphocytes and cause immune dysfunction in COVID-19.

KEYWORDS

apoptosis, CD8⁺ T cells, COVID-19, lymphopenia, phosphatidylserine, platelet-derived microparticle, SARS-CoV-2, thromboinflammation

1 | INTRODUCTION

The recently emerged human pathogenic severe acute respiratory syndrome coronavirus 2 (SARS-CoV-2) causes various clinical syndromes, summarised under coronavirus disease-2019 (COVID-19). The excessive inflammatory response associated with COVID-19 can cause severe complications such as acute respiratory distress syndrome, septic shock and multi-organ failure (Guan et al., 2020; MacLaren et al., 2020; Wölfel et al., 2020). A significant cause of morbidity and mortality in COVID-19 patients is 'thromboinflammation'. Although not fully understood, inflammation through complement activation and cytokine release, platelet overactivity and apoptosis (thrombocytopenia), as well as coagulation abnormalities (coagulopathy) play critical roles in this complex clinical picture (reviewed in Gu et al. (2021)).

Similar vascular complications occur in the antiphospholipid syndrome, where autoantibodies target phosphatidylserine (PS)/prothrombin complexes (Corban et al., 2017). This syndrome may manifest itself in COVID-19 patients (Zhang et al., 2020), linking PS to thromboinflammation. PS is a plasma membrane component actively retained by an ATP-requiring process at the inner membrane surface in living cells. PS retention stops, for example, during cell death or when cells release PS-containing microparticles or enveloped viruses. Then PS relocates to the outer layer of the cell membrane, where it can interact with extracellular proteins, including coagulation and complement systems. PS activates the alternative and the classical complement pathways (Mevorach et al., 1998; Tan et al., 2010; Wang et al., 1993) by binding to complement C3 (Huong et al., 2001), C3bi (Mevorach et al., 1998) and C1q (Païdassi et al., 2008). Activated platelets release platelet-derived microparticles (PMPs), which cause thrombin formation, coagulation, activation of the complement system, and inflammation in a PS-dependent manner (Melki et al., 2017; Owens & Mackman, 2011; Ridger et al., 2017).

Patients with severe COVID-19 also show striking immune dysregulation, the reasons for which are not entirely understood. A direct correlation between blood clotting components and the immune response exists (Su et al., 2020). Various immune abnormalities such as increased inflammatory cytokines (Del Valle et al., 2020), immune cell exhaustion (Zheng et al., 2020) and general lymphopenia (Cao, 2020; Chen et al., 2020; Huang et al., 2020; Liu et al., 2020; Yang et al., 2020,) correlate with disease severity (Mathew et al., 2020). T cell lymphopenia (Laing et al., 2020), probably caused by excessive apoptotic T cell death similar to sepsis (Hotchkiss & Nicholson, 2006), is of particular relevance as SARS-CoV-2-specific T cell responses control and resolve the primary infection (Liao et al., 2020; Rydzynski Moderbacher et al., 2020; Sekine et al., 2020; Zhou et al., 2020). In fatal COVID-19, the adaptive immune response starts too late (reviewed in Sette and Crotty (2021)), while its rapid onset would be highly beneficial (Braun et al., 2020; Rydzynski Moderbacher et al., 2020; Tan et al., 2020). However, the reasons and precise mechanisms for adaptive immune disturbance, lymphopenia and thromboinflammation in COVID-19 remain poorly defined.

To investigate these aspects of COVID-19 in more detail, we interrogated PBMC of 54 patients from the COVID-19 Registry of the LMU Munich (CORKUM) and 35 healthy and 12 recovered donors between April 2020 and February 2021. We performed image flow cytometry (IFC) and image analysis by deep learning algorithms (Kranich et al., 2020) using highly sensitive reagents specific for PS (Kranich et al., 2020; Trautz et al., 2017). COVID-19 blood samples contained abnormally high numbers of PS⁺ peripheral blood mononuclear cells (PBMC). Although PS is a marker for dying cells, nearly all PS⁺ cells were living cells associated with PS⁺CD41⁺ PMPs or larger PS⁺CD41⁺ platelet fragments. The grade of PS⁺ PMP-associated PBMC correlated with lymphopenia and disease severity, showing a higher correlation than commonly used laboratory diagnostic markers such as IL-6, D-Dimer (Mathew et al., 2020) and C-reactive protein (CRP) (Li et al., 2020). PS⁺ PMPs were strongly associated with dividing effector CD8⁺ T cells with upregulated expression of cell-cycle genes. Fractions of T cell-associated PS⁺ PMPs carried CD274 (PD-L1), which could impact the survival of T cells and potentially contribute to functional inhibition and lymphopenia. As PS⁺ PMPs remained associated with PBMC several weeks after the initial SARS-CoV2-diagnosis, they might sustain the adverse inflammatory and prothrombotic effects over a long time and contribute to the complex clinical picture of thromboinflammation (reviewed in (Gu et al., 2021; Lind, 2021)). Together, our findings reveal an extensive association of PS⁺ PMPs with lymphocytes as a novel marker to classify COVID-19 disease severity and a potentially relevant contributor to thromboinflammation and lymphocyte dysfunction.

2 | RESULTS

2.1 | PBMC from COVID-19 patients show substantial PS surface exposure

To test if immune cell death rates were elevated during COVID-19, we analysed peripheral blood mononuclear cells (PBMC) of COVID-19 patients and compared them to those from healthy and recovered donors. Table S1 show clinical metadata for our cohort of COVID-19 patients and control groups. One hallmark of apoptotic cell death is the PS exposure on the outer membrane surface of cells. To reveal PS on PBMC, we utilised recombinant Milk fat globule-EGF factor 8 protein (MFG-E8) derived recombinant proteins, which bind PS under physiological conditions with high sensitivity on apoptotic cells and subcellular PS⁺ extracellular vesicles (EVs) (Kranich et al., 2020; Trautz et al., 2017). Flow cytometry results showed that the frequencies of PS⁺ cells in blood from all COVID-19 patients were significantly higher than in PBMC from healthy or recovered donors (Figure 1a). To analyse if this data can classify patients according to disease severity, we employed the World Health Organization's (WHO) eight-point ordinal scale for COVID-19 trial endpoints (WorldHealthOrganization, 2020) (Figure 1b). In our patient cohort, the scores WHO 2 and WHO 7 were absent. We combined WHO scores into 'mild' (WHO 1–3), 'moderate' (WHO 4) and 'severe' (WHO 5–8) groups for the subsequent analyses. Additionally, we also included a group of healthy donors (HD, $n = 30$) and recovered patients ($n = 12$, >69 days post 1st SARS-CoV-2⁺ diagnosis by PCR, either never hospitalised or released from the hospital with WHO score 1–2). The frequencies of PS⁺ PBMC increased with severity of COVID-19 disease in the following order: healthy controls (WHO 0) < recovered patients < WHO 1–3 (mild) < WHO 4 (moderate) < WHO 5–8 (severe) (Figure 1c). In severely diseased patients, 30%–90% of all PBMC were PS⁺ (Figure 1c). Accordingly, the individual WHO scores positively correlated with high significance with the frequencies of PS⁺ PBMC of COVID-19 patients. Importantly, the correlation of PS⁺ PBMC against WHO_{max} was much stronger than against the WHO score at sampling time (Figure S1A and 1d).

In order to assess whether the frequency of PS⁺ PBMCs is an independent predictor for a severe disease outcome such as ventilation requirement (Figure 1e) or death (Figure 1f) within our cohort, we performed an area under the receiver operating characteristic curve (AUROC) analysis. Frequency of PS⁺ PBMC was better for predicting ventilation requirement (AUC 0.760, threshold 41.15, specificity 0.53, sensitivity 0.91; Figure 1e) and death (AUC 0.907, threshold 43.525, specificity 0.90, sensitivity 0.83; Figure 1f) than C-reactive protein (CRP), D-Dimer, Ferritin, Fibrinogen, international normalised ratio (INR), partial thromboplastin time (PTT) or number of platelets (Figure S1B and C). Only IL-6 had better prediction scores for ventilation requirement (AUC 0.841, threshold 19.975, specificity 0.71, sensitivity 0.87; Figure 1b) and death (AUC 0.949, threshold 45.05, specificity 0.80, sensitivity 1; Figure S1C). Kaplan-Meier curves show that patients with a frequency of PS⁺ PBMCs higher than 41.15% or 43.53% had a higher incidence of requiring ventilation or succumbing to disease, respectively (Figure 1e). However, our study was an exploratory study with a limited number of patients. Therefore, the predictive capacity of the frequency of PS⁺ PBMCs needs to be validated in a larger cohort.

The blood sampling time points differed within our patient cohort due to organisational reasons. We investigated whether the sampling time point would affect the results and performed PS measurements at several time points for selected patients. These data show that although the frequencies of PS⁺ PBMCs show some variability, we detected strongly elevated levels for up to 30 days (Figure 2A). In contrast, in recovered patients, PS⁺ PBMC returned to the levels of healthy controls. To further assess the influence of sampling time and PS⁺ PBMC frequency, we performed a Spearman correlation test with time since the first diagnosis (FD) or time since symptom onset and found no correlation with PS⁺ PBMC frequencies (Figure S2B). Furthermore, there was also no correlation between the frequency of PS⁺ PBMC and age in healthy donors or recovered patients (Figure S2C).

In summary, the number of PS⁺ PBMC in the blood of COVID-19 patients represents a new parameter that correlates strongly with disease severity.

2.2 | PBMC in COVID-19 patients are associated with PS⁺ EVs, and the amount correlates with the severity of the disease

PS exposure occurs on various cells and cell-derived microparticles, including tumour cells, erythrocytes, neutrophils, monocytes, endothelial cells, activated platelets and PMPs. PS-exposure is a significant regulator of the blood coagulation system (reviewed in Connor et al. (2010)). We have recently shown that most PS⁺ cells in the spleen of virus-infected mice are not dying, but cells carried PS⁺ EVs (Kranich et al., 2020). To determine whether PS⁺ PBMC in COVID-19 patients were apoptotic cells contributing to the described lymphopenia or EV⁺ cells, we analysed the images of PS⁺ PBMC acquired by IFC. Some cells showed almost entirely PS⁺ cell bodies with strongly labeled apoptotic blebs, typical for cell death (Figure 2a). These cells still have an intact cell membrane since they did not stain with the live/dead dye used to exclude necrotic cells from the analysis. However, we also detected many cells with the characteristic round brightfield image morphology of living cells, with only one or a few intensely PS⁺ structures of subcellular size (Figure 2a). These particles resembled cell-associated PS⁺ EVs, which we recently identified in virus-infected mice (Kranich et al., 2020). We next used a machine learning-based convolutional

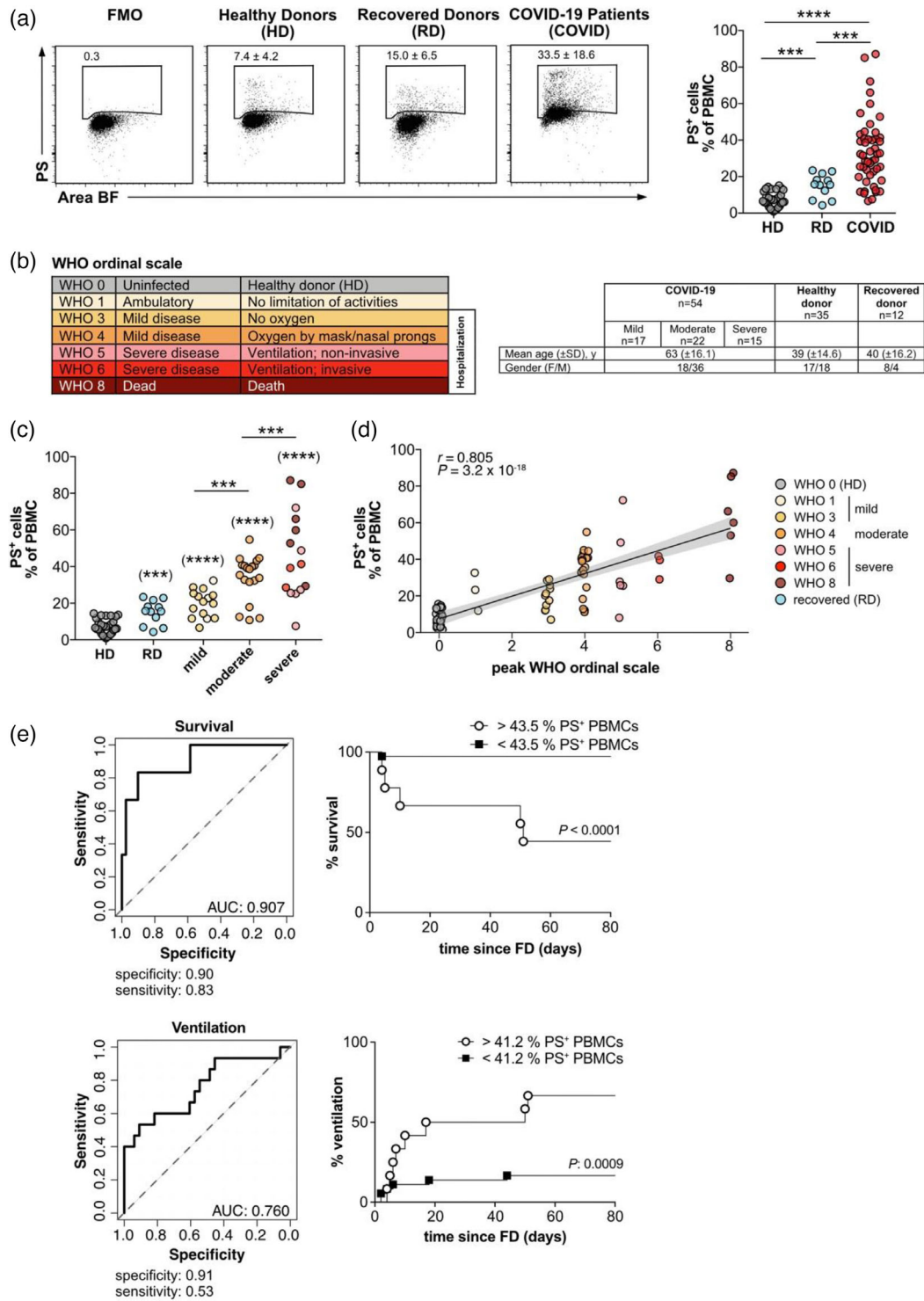


FIGURE 1 The frequencies of PS⁺ PBMC from COVID patients correlates with disease severity. (a) PBMC from COVID-19 patients (COVID), healthy donors (HD) and recovered donors (RD) were stained for PS and analysed by flow cytometry. Numbers in dot plots correspond to the percentage of PS⁺ cells in the gate shown. The right-hand graph shows the summary of all percentages. (b) Overview of WHO ordinal scale and colour code used. Table shows the number, age and gender of the different study groups. (c) Grouped analysis of the data from (a). (d) Same as (c), but plotted against the WHO ordinal scale ($n = 38-79$). PS⁺ PBMCs correlate with the severity of the disease. The plot shows the Spearman correlation test and linear regression line with 95% confidence interval shading (A, C, D: HD, $n = 30$; RD, $n = 12$; COVID, $n = 49$). Significance in (a) and (c) was determined by Mann-Whitney test: * $p < 0.05$, ** $p < 0.01$, *** $p < 0.001$ and **** $p < 0.0001$. Asterisks in brackets show statistically significant differences as compared to HD. FMO: Fluorescence minus one control; Area BF: Area bright field. (e) ROC curve analysis of PS⁺ PBMCs from COVID-19 patients ($n = 49$) for predicting survival (upper plot) and ventilation (lower plot). AUC values (95% CI) (left hand panels) and Kaplan-Meier survival and ventilation curves of patients grouped according to the indicated PS⁺ PBMCs-thresholds (right hand panels) are shown. Time represents the number of days from first diagnosis (FD). Optimal cut-off values for % PS⁺ PBMCs were determined by ROC analysis and used to define the two groups. First measured values of % PS⁺ PBMCs were used for analysis. Significance was determined by Log-rank test

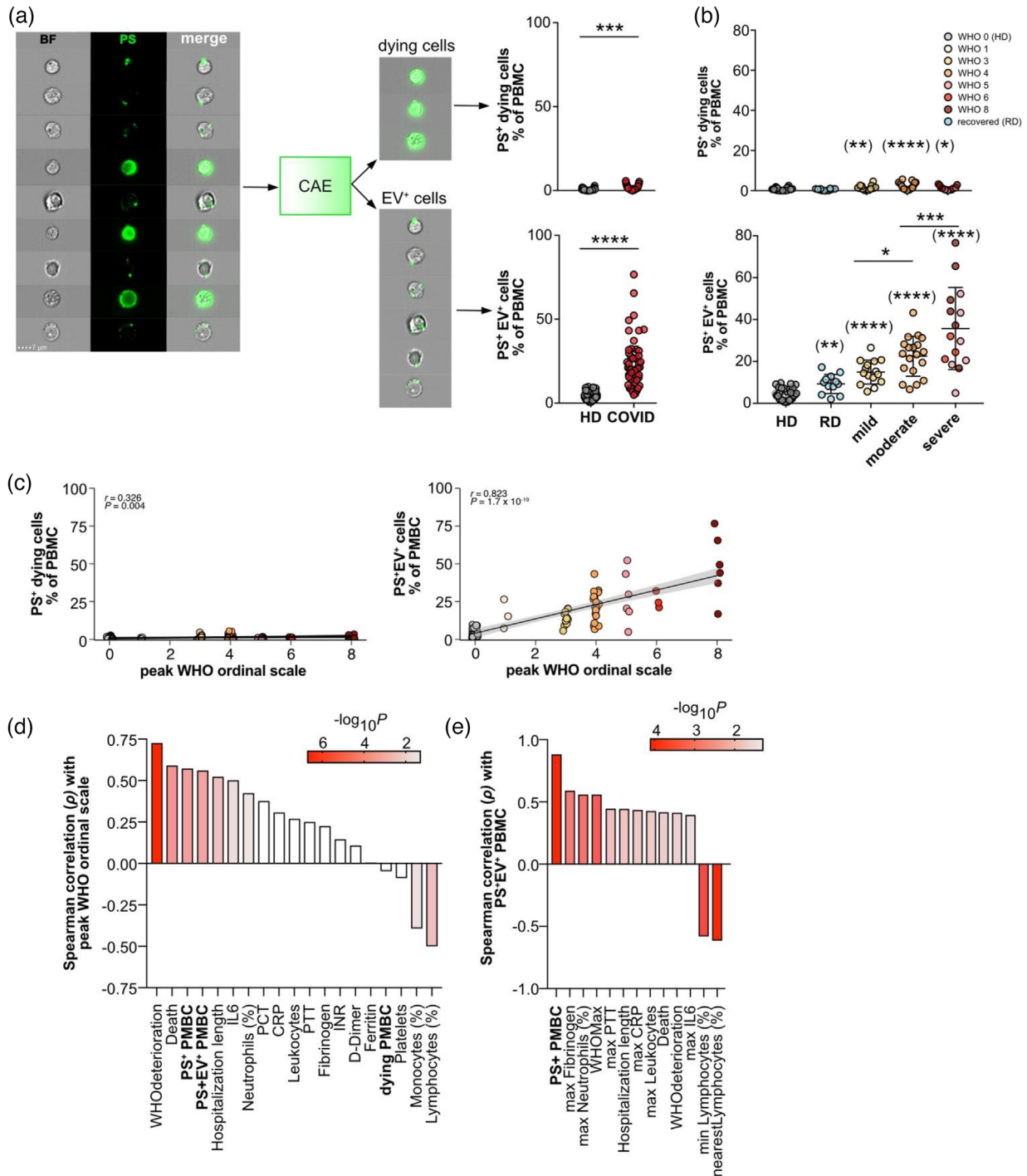


FIGURE 2 EV⁺ cells, but not dying cells from COVID-19 patients correlate with disease severity. (a) PBMC from healthy donors (HD, $n = 30$) and COVID ($n = 49$) were analysed by imaging flow cytometry (IFC). To discriminate dying and EV⁺ cells, PBMC were analysed using IDEAS, CAE and FlowJo. PS⁺ cells were gated, and their TIF images (16-bit, raw) exported using the IDEAS software. CAE results with the classification dying/EV⁺ were re-imported into IDEAS, and separate FCS files containing all cells or only PS⁺/dying cells and PS⁺/EV⁺ cells were generated for further analysis in FlowJo. Dying (a, upper panel) and EV⁺ (a, lower panel) cells are shown as % of PBMC. (b) Results from a) are plotted against groups HD ($n = 30$), RD ($n = 12$), mild ($n = 15$), moderate ($n = 19$) and severe disease ($n = 15$) for dying cells (upper panel) and EV⁺ cells (lower panel). (c) Plotting of the data from (b) against WHO ordinal scale. The plot shows the Spearman correlation test and linear regression line with 95% confidence interval shading ($n = 38-79$). (d) Summary of correlations of selected ‘nearest’ ($n = 23-49$) laboratory and clinical parameters with peak WHO ordinal scale or and selected (e) our measurements of PS⁺, PS⁺EV⁺ and dying cells (bold) ($n = 23-49$). Significance was determined by Mann-Whitney test: * $p < 0.05$, ** $p < 0.01$, *** $p < 0.001$ and **** $p < 0.0001$. Asterisks in brackets show statistically significant differences as compared to HD

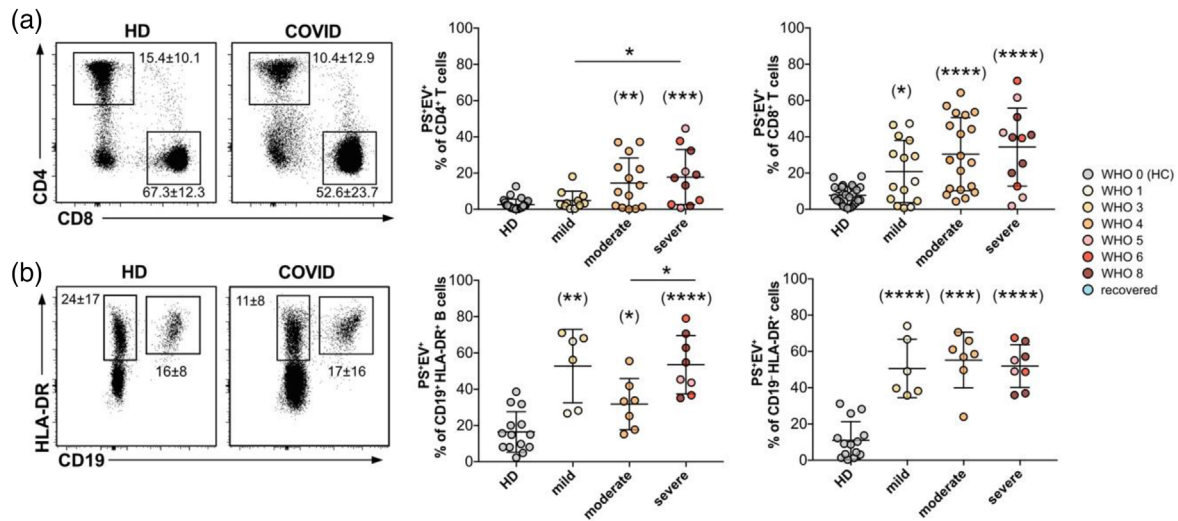


FIGURE 3 Identification of EV⁺ cells in PBMC from COVID-patients and healthy donors. PBMC were analysed by IFC (gating strategy shown in Figure S3A and B). PS⁺ CD4⁺ and CD8⁺ T cells (a) and CD19⁺ HLA-DR⁺ B cells and CD19-HLA-DR⁺ cells (containing mainly dendritic cells, monocytes) (b) were classified as PS⁺EV⁺ using the CAE and their total frequencies were plotted against HD (B, $n = 14$; A, CD4, $n = 24$; a, CD8, $n = 27$), mild (b, $n = 6$; A, CD4, $n = 11$; A, CD8, $n = 15$), moderate (B, $n = 7$; a, CD4, $n = 14$; A, CD8, $n = 19$), severe (b, $n = 8$; a, CD4, $n = 11$; a, CD8, $n = 12$) disease groups. Numbers next to the gates show the mean percentage \pm SD of all cells depicted inside the dot plot that lie within the respective gate, while the graphs show the average frequency \pm SD of EV⁺ cells within the analysed subpopulation. Significance was determined by Mann-Whitney test: * $p < 0.05$, ** $p < 0.01$, *** $p < 0.001$ and **** $p < 0.0001$. Asterisks in brackets show statistically significant differences as compared to HD

autoencoder (CAE) to group PBMC into bona fide PS⁺ dying cells or cells associated with PS⁺ EVs (Figure 2a), as previously validated (Kranich et al., 2020). After training with pre-defined images of PS⁺ dying or PS⁺ EV-associated cells, the CAE algorithm digitally sorts PS⁺ cells into both categories with high precision (Figure 2a). When we analysed the CAE-classified PS⁺ dying cells and PS⁺EV⁺ cells separately (Figure 2a), we found that the majority of PS⁺ PBMC contained live cells associated with PS⁺ EV-like structures rather than PS⁺ dying cells (Figure 2b). Despite the rarity of dying cells, patients with the score WHO 4 showed the highest frequencies (Figure 2b, upper panel). Furthermore, only PS⁺EV⁺ PBMC, not PS⁺ dying cells, classified the patients into disease score groups 'mild' (WHO 1–3), 'moderate' (WHO 4), and 'severe' (WHO 5–8) and separated them clearly from HD and recovered patients (Figure 2b, lower panel). Similarly, PS⁺EV⁺ PBMC, but not PS⁺ dying cells, showed a highly significant correlation with WHO scores (Figure 2c). Several laboratory values that are either increased (leukocytes, IL-6, neutrophils, procalcitonin (PCT), C-reactive protein (CRP), partial thromboplastin time (PTT), D-dimer, etc.) or decreased (lymphocytes) were shown to indicate an unfavorable progression of COVID-19 disease (Lippi & Plebani, 2020).

We confirmed these correlations in our patient cohort (Figure S4A). The frequencies of PS⁺EV⁺ and PS⁺ PBMC ranked in the top groups of measurements among inflammatory and coagulation parameters such as IL-6, PCT, CRP, PTT, D-Dimer and others (Figure S4A). The strongest negative correlations existed with low lymphocyte counts (Figure S4A). For better comparability, we focussed next only on those values determined from the same blood draw or close to our PS-measurements ('nearest values' in Figure S4A, shown in Figure 2d). Here, both PS⁺EV⁺ PBMC and PS⁺ PBMC correlated better than all other blood parameters with peak WHO ordinal scale (Figure 2d). Moreover, PS⁺EV⁺ PBMC frequencies correlated strongly with parameters of coagulation (fibrinogen, PTT), inflammation (IL-6, CRP) and lymphopenia (lymphocyte counts) (Figure 2e and S4B).

As the frequencies of PS⁺ PBMCs in the blood of COVID-patients turned out to be an independent predictor for a severe disease outcome (Figure 1e), we now wondered if PS⁺EV⁺ PBMCs, which constituted the major part of this population, allows such a prediction. Indeed, the AUROC analysis showed comparable prediction values for ventilation requirement (AUC 0.791, threshold 29, specificity 0.91, sensitivity 0.60) and death (AUC 0.866, threshold 31.4, specificity 0.88, sensitivity 0.83) (Figure S1D). Therefore, our new type of PS analysis allows the detection of subcellular particles associated with PBMC of COVID-19 patients. The percentage of PBMC bound to these PS⁺ particles correlated with the maximal (peak) WHO score of COVID-19 patients and allowed to classify patients with higher significance than some of the previously established medical laboratory parameters (Lippi & Plebani, 2020).

2.3 | PS⁺ EVs bind to several PBMC populations

Next, we investigated whether PS⁺ EVs would selectively associate with specific PBMC subpopulations. We examined CD4⁺ and CD8⁺ T cells (Figure 3a), CD19⁺ B cells (Figure 3b) and HLA-DR⁺CD19⁻CD3⁻ PBMC (containing mainly monocytes and

dendritic cells as central blood populations, Figure 3b). In general, CD8⁺ T cells were more strongly associated with PS⁺ EVs than CD4⁺ T cells (Figure 3a). However, both T cell subsets showed a similar tendency of increased PS⁺ EV binding in patients with a higher WHO score (Figure 3a). B cells and blood monocyte-containing populations of patients in the different WHO groups were also associated relatively strongly with PS⁺ EVs (Figure 3b). However, there was no actual grading with the severity of the disease. In summary, most blood cells showed a strong association with PS⁺ EVs in the patients. The frequency of PS⁺ EV⁺ CD8⁺ T cells best reflected the severity of COVID-19 disease.

2.4 | PS⁺ EVs associated with PBMC from COVID-19 patients are PS⁺CD41⁺ platelet-derived microparticles

EVs classify according to their size and origin into exosomes (up to 150 nm), microvesicles or microparticles (MPs; 100–1000 nm) and apoptotic EVs or apoptotic bodies (100–5000nm) (Mathieu et al., 2018). To better characterise the EVs associated with lymphocytes in COVID-19 patients, we isolated PS⁺ lymphocytes (B and T cells, PS⁺CD19⁺CD3ε⁺) from COVID-19 patients by FACS. We used recombinantly expressed, biotinylated MFG-E8-derived PS-binding domain mCl, which was multimerised by streptavidin (SA) (mCl-multimer/SA-APC) for PS-detection by flow cytometry (Figure S3C) and mCl-multimer/SA-gold for PS-detection by subsequent transmission electron microscopy (TEM). TEM pictures show cell-associated particles of a subcellular size bound to lymphocytes, which morphologically resemble T cells (Figure 4a–f). Many (Figure 4b, d, and f, open white arrows), but not all EVs (Figure 4c, arrows), were PS⁺, and most EVs were >100 nm in size (Figure 4b, d and f). The particles were mainly round and had different shapes and contained other smaller components, cell contents or organelles (Figure 4b, d, white star). However, we also found PS⁺ tubular elongated structures (Figure 4d, black star). Relatively large particles with highly diverse shapes, including tubular shapes and content are known features of PMPs, 50% of which are PS positive (Arraud et al., 2014; Ponomareva et al., 2017; Reininger et al., 2006). Hyperactivated platelets in COVID-19 patients (Teuwen et al., 2020) are sources for PMPs and contribute to the hypercoagulability state of the disease (Klok et al., 2020; Middeldorp et al., 2020; Tang et al., 2020). Activated platelets can release two types of EVs, (i) smaller exosomes (40–100 nm in diameter) derived by exocytosis from α-granules and the multivesicular body, and (ii) PS⁺ MP (100–1000 nm in size), formed by budding of the plasma membrane (Aatonen et al., 2014; Heijnen et al., 1999). These similarities let us hypothesise that PMPs attach to PBMC of COVID-19 patients.

To test this hypothesis, we stained PBMC from COVID-19 patients for CD41, a platelet marker, part of a fibrinogen-receptor and present on platelet-derived PMPs (Heijnen et al., 1999) (Figure S5 and 4g). Analysis of flow cytometry data of PBMC confirmed our assumption and showed that many PBMC were positive for the platelet marker CD41 (Figure 4g). However, CD41 could not distinguish PBMC from healthy donors and COVID because CD41⁺ PBMC also existed in healthy donors (Figure 4g, CD41⁺). In contrast, PS-positivity alone distinguished PBMC from healthy donors and COVID-19 patients, as PS⁺ PBMC were highly significantly enriched in patients (Figure 4g, PS⁺).

To analyse PS and CD41 and their possible colocalisation, we performed image analysis of PBMC (Figure S5A, B) and T lymphocytes (Figure 4h and i). In COVID-19 patients, we observed a substantial increase of PS⁺CD41⁺ PBMCs and T cells from 7% to 25% and from 2% to 18%, respectively. The increase in CD41[−]PS⁺ cells was not as pronounced but still significant (Figure 4h and i, Figure S5A and B). This finding shows that most PS⁺ cells acquire PS through the binding of CD41⁺ platelets or their PMPs. To investigate whether the cells preferentially bind whole platelets or smaller PMPs, we quantified CD41^{hi} versus CD41^{low} cells. The CD41^{hi} gate contained mainly cells with large CD41⁺ particles attached, which were also visible in the brightfield (BF) channel – presumably whole platelets. In contrast, the cells in the CD41^{low} gate were associated with small, more dimly stained spots that were too small to be visible in the BF channel – presumably PMPs (Figure 4i). While T cells very clearly had a strong preference for PMP binding (15% of CD3⁺ T cells were CD41^{low} and 2% CD41^{hi}, Figure 4i), PBMCs did not show such a clear preference (approx. 15% were CD41^{low}, 9% were CD41^{hi}, Figure S5C). Our data show that PBMCs from COVID-19 patients associate to a high degree with PS⁺ platelets and PMPs, while T cells rarely bind whole platelets, but rather PMPs.

2.5 | PMPs carry markers of activated platelets

SARS-CoV-2-infection causes platelet activation and alters their functions (Manne et al., 2020; Zaid et al., 2020). The results of our study suggested that the PMPs associated with lymphocytes in COVID-19 patients originate from activated CD41⁺ platelets. In addition to PS and CD41, markers such as CD62P (P-selectin) and the tetraspanin CD63 are present on PMPs derived from activated platelets (van der Zee et al., 2006). Our patient cohort showed increased percentages of PS⁺ and CD62P⁺ platelets, both markers for platelet activation (Figure 6a–c), although the increase in CD62P⁺ platelets did not reach statistical significance. When associated with CD8⁺ T cells, platelet-derived molecules PD-L1 (CD274) (Rolfes et al., 2018) and CD86 (Chapman et al., 2012) on PMPs could be potentially negative or positive costimulatory triggers, respectively. Platelets were strongly positive for CD274 (Figure S6B and C), but this was not different between healthy donors and patients (Figure S6B). The same was true for CD86, which we found in similar amounts and generally only very few platelets that were positive for this molecule in both

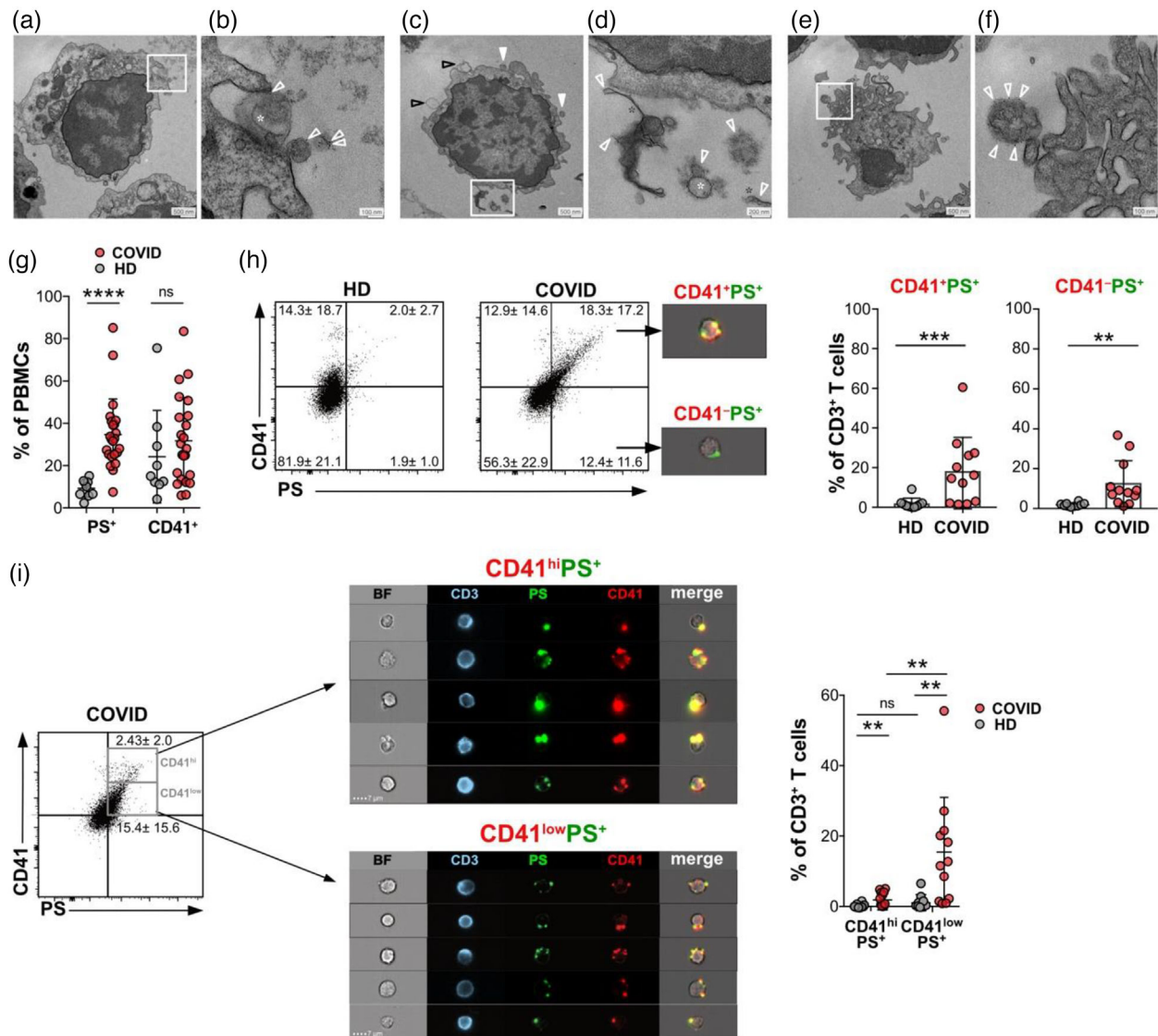


FIGURE 4 Structural and phenotypic characterisation of EVs associated with lymphocytes from COVID patients. Patient parameters for these experiments are depicted in Table S3. PS⁺ CD3^ε⁺ T and CD19⁺ B lymphocytes were isolated from PBMC of COVID patients (WHO_{max} score 3) by FACS-sorting (Figure S3C) and subsequently labeled with mCl-multimer/streptavidin-gold for TEM analysis of PS and analysed structurally by TEM (a-f). (b, d, f) represent the magnified sections (white frame) of (a, c, e), respectively. Open white arrowheads (b, c, f) mark PS labelling by mCl-multimer/streptavidin-gold; arrowheads in C point to PS⁻ EVs; white star (b, d) or black star (d) marks organelle-like structures within EVs, or PS⁺ tubular elongated structures (d), respectively. Analysis of platelet marker CD41 on T cells. (g) PBMC were analysed as shown in Figure S3 (HD, *n* = 11; COVID, *n* = 23) for PS and CD41. (h) CD3^ε⁺ T lymphocytes (gated as in Figure S3D) were stained for CD41 and PS and analysed by IFC (HD, *n* = 10; COVID, *n* = 12). Images represent cells of the respective quadrants. Numbers are the percentage of cells with the respective quadrants and are shown also in the bar graphs. (i) Percentage of T cells in the quadrants of PS⁺ CD41^{hi} and PS⁺ CD41^{low} CD3^ε⁺ T cells. Dot plots show the gating of PS⁺ CD41^{hi} and PS⁺ CD41^{low} CD3^ε⁺ T lymphocytes. IFC images show representative cells of the CD41^{hi} and CD41^{low} gates. The bar graph shows the frequency of PS⁺ CD41^{hi} and PS⁺ CD41^{low} T cells as percent of all CD3^ε⁺ T cells. Statistical significance was determined by paired Wilcoxon test and is indicated by asterisks (ns *p* > 0.5; **p* ≤ 0.05; ***p* ≤ 0.01; ****p* ≤ 0.001; two-tailed unpaired *t*-test)

groups (Figure S4B and C). We evaluated next if PS⁺EV⁺ CD8⁺ T cells were positive for these platelet markers. PS⁺EV⁺ CD8⁺ T cells showed significantly increased mean fluorescence intensities (MFI) for platelet markers CD41, CD63, CD62P and CD274 compared to their PS⁻ counterparts (Figure 5a and b). The frequency of T cells, which were positive for these markers, was also increased in PS⁺EV⁺ T cells (CD41, CD63, CD62P; Figure 5b). This finding indicated that PMPs carried the surface molecules of their activated 'parent' platelets to the surface of activated CD8⁺ T cells in COVID-19 patients. When we analysed the images of CD41, CD63, CD274 and CD62P stained T cells, we also observed an EV-like staining pattern of these markers, similar to the PS staining (Figure 5c).

To confirm that these markers originate from activated platelets or their PMPs, we quantified PMP-marker colocalisation with PS. We used the bright detail similarity (BDS) feature to quantify the pixel overlap of PS⁺ and PMP-marker⁺ spots identified

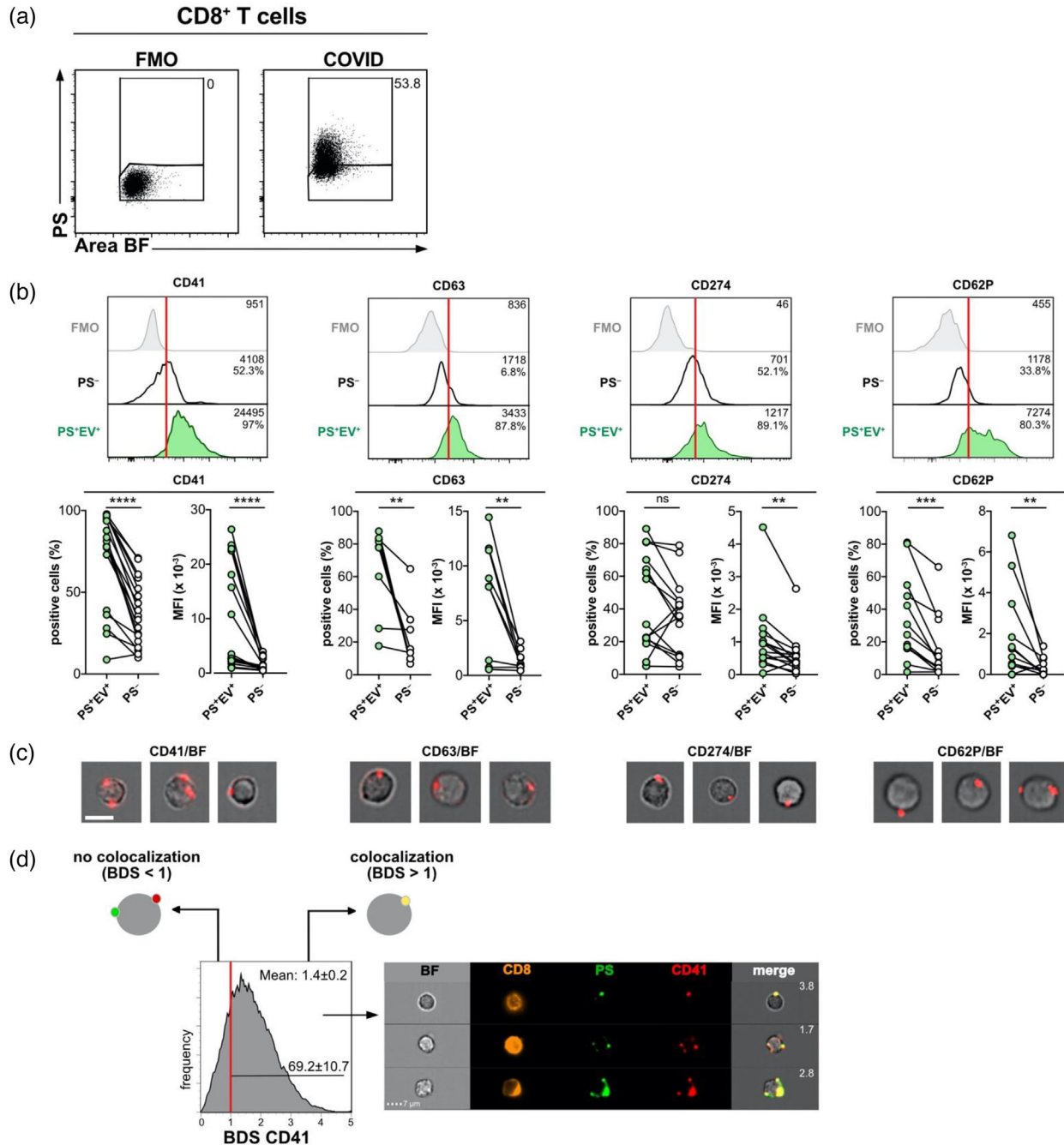


FIGURE 5 EVs bound to CD8⁺ T cells originate from platelets and PMP markers colocalise with PS⁺ EVs. Patient parameters for these experiments are depicted in Table S4. (a) Analysis of CD8⁺ T cells of COVID patients (CD41, *n* = 18; CD63, *n* = 9; CD274, *n* = 15, CD62P, *n* = 13) were gated as shown in Figure S3E and then further separated into PS⁺EV⁺ and PS⁻ T cells. Numbers represent the percentage of cells within the gates. (b) Then cells were analysed separately for expression of platelet-markers CD41, CD63, CD62P and CD274. Median fluorescence intensities (MFI) ± SD of these proteins and % of positive cells are indicated in the histograms. Summaries of all results are shown below histograms. (c) Representative images of CD41⁺, CD63⁺, CD62P⁺ and CD274⁺ CD8⁺ T cells show the EV-like staining pattern of these markers. (d) Colocalisation analysis between PS and PMP-marker staining. To identify PS⁺ spots the Dilate(Peak(M02, PS, Bright, 5),1) and to identify PMP-marker⁺ spots the Dilate(Peak(M_{marker},marker channel, Bright, 1),1) masks were used. To quantify the degree of colocalisation between these masks, bright details similarity scores (BDS) were calculated. Cells with a BDS < 1 did not show any significant colocalisation as determined by visual inspection. Cells with a BDS > 1 showed substantial colocalisation of PS and the respective platelet marker. BDS scores are shown in the representative example images. Histograms show the BDS scores of PS⁺EV⁺ CD8⁺ cells. The mean BDS score and the percentage of cells showing colocalisation (BDS > 1) are indicated within histograms. Statistical significance was determined by paired Wilcoxon test and is indicated by asterisks (ns *p* > 0.5; **p* ≤ 0.05; ***p* ≤ 0.01; ****p* ≤ 0.001)

using a peak mask in the IDEAS software (Figure 5d). As determined by visual inspection, BDS values >1 indicate substantial colocalisation between PS and other markers. This analysis showed that the great majority of all PS⁺EV⁺ CD8⁺ T cells (64%–82%) showed strong colocalisation of PS⁺EVs with CD41 (Figure 5d), CD63, CD62P or CD274 (Figure S8) with average BDS scores ranging from 1.3 to 1.8 (Figure 5 and S8). These results indicate that most of the PMPs attached to CD8⁺ T cells originate from activated platelets and carried platelet markers. Furthermore, since human T cells do not express markers like CD41 and CD62P, it excludes the possibility that the PS⁺EVs attached to T cells originate from T cells themselves or mark eventual focal PS⁺ regions on the T cell surface membrane.

2.6 | PS⁺CD41⁺ PMPs are preferentially bound to proliferating CD8⁺ T cells

Next, we wanted to assess whether there are functional differences between PMP⁺ and PMP⁻ CD8⁺ T cells. For this, we performed RNAseq analysis of FACS-sorted PS⁺ and PS⁻ non-naïve CD8⁺ T cells from peripheral blood of 4 patients (Figure 6a and Figure S3G). Despite heterogeneity between patients, we could identify gene sets that showed clear enrichment in PS⁺ (Figure 6b) and PS⁻ T cells (Figure 6c). Table S5 shows a summary of the gene set enrichment analysis (GSEA) against 4597 datasets in the gene ontology (GO) database.

PS⁺ CD8⁺ T cells had enriched genes controlling cell cycle and division, with normalised enrichment scores (NES) of 2.24 and 2.70 for the gene ontology biological process (GOBP) ‘cell division’ and KEGG ‘cell cycle’ gene sets, respectively. Among the genes upregulated in PS⁺ CD8⁺ T cells of all patients were several cell division control (CDC) genes, such as CDC45, CDCA8, CDC20, CDC6 or transcription factors E2F7 and E2F2, which are involved in cell cycle regulation (DeGregori & Johnson, 2006). Also, Birc5 (survivin) which plays a crucial role in costimulation-driven clonal expansion of T cells (Song et al., 2005), was upregulated in all patients.

Cells in the G2/M phase exhibit a general inhibition of translation (Sachs, 2000). Hence, the reduced expression of genes initiating translation in PS⁺ CD8⁺ T cells is in line with the observed upregulation of proliferation-associated genes (Figure 6c).

Although PS⁻ and PS⁺ CD8⁺ T cells had few apparent differences in gene expression due to the high degree of variability between individual patients, it is striking that binding of PS⁺ PMPs was associated with increased proliferation. To confirm the RNAseq results, we stained CD8⁺ T cells with the proliferation marker Ki-67, which labels dividing and recently dividing cells in G1, S, G2 and M phase, but is absent in resting cells (Scholzen & Gerdes, 2000) and compared the frequency of PS⁻ and PS⁺EV⁺ Ki-67⁺ cells. PS⁺EV⁺ CD8⁺ T cells (Figure 6d and e) and PS⁺EV⁺ CD4⁺ T cells (Figure S8) contained significantly more Ki-67⁺ proliferating cells than their PS⁻ T cell counterparts from the same patient. In both cases, Ki-67 staining localised to the nucleus and PS⁺ PMPs to the periphery of the same cells (Figure 6e and S8B). Our results indicate that PS⁺ PMPs preferentially bind to proliferating T cells and may affect T cells in this cycling stage.

We were also interested to find out, whether CD8⁺ T cells binding PS⁺ PMPs exhibit an effector or memory phenotype. Previous reports showed a high prevalence of SARS-CoV-2-specific T cells mainly among T cells with phenotypes of effector memory (T_{EM}) and terminal effector memory cells reexpressing CD45RA (T_{EMRA}) cells (Kared et al., 2021). We did not observe a clear enrichment of effector or memory genes (Best et al., 2013). However, we found an upregulation of effector-associated genes, such as CXC Motif Chemokine Receptor 3 (Cxcr3), Interferon γ (Ifng), Granzyme A and B (Gzma and Gzmab) and CC-chemokine ligand 5 (Ccl5) in PS⁺ CD8⁺ T cells of all four patients. In contrast, memory-related genes, such as C-X-C Motif Chemokine Receptor 4 (Cxcr4), DNA-binding protein inhibitor ID-3 (Id3) and interleukin-7 receptor (Il7r), showed a subtle downregulation in all patients. These findings indicate that PMP-associated CD8⁺ T cells are proliferating effector cells rather than memory cells. This we also confirmed with flow cytometry using CCR7 and CD45RA as markers (Sallusto et al., 2004). We found PS⁺PMPs preferentially associated with CCR7⁻CD45RA⁻ CD8⁺ T_{EM} cells and terminally differentiated CCR7⁻CD45RA⁺ CD8⁺ T_{EMRA} (Figure S9).

Our novel analysis method allows the detection of dying as well as PS⁺ EV-associated living cells (Figure 2). We next wanted to analyse whether the apoptosis rate of CD8⁺ T cells would be elevated in COVID-19 patients as compared to healthy donors and could contribute to the observed T cell lymphopenia (Laing et al., 2020). To this end, we quantified the number of CD8⁺ T cells classified as apoptotic by the CAE algorithm (Figure S10). The CD8⁺ T cell apoptosis rate was significantly increased in moderate and severe cases compared to healthy donors (Figure S10A and B). This increased rate of apoptosis might ultimately contribute to T cell loss and lymphopenia.

Taken together, we present a robust method, which allows the detection of dying as well as PS⁺EV⁺-associated living cells within PBMCs of COVID-19 patients in a single step. This type of analysis might help understand events that directly affect the immune system and might be caused by EV-immune cell interactions.

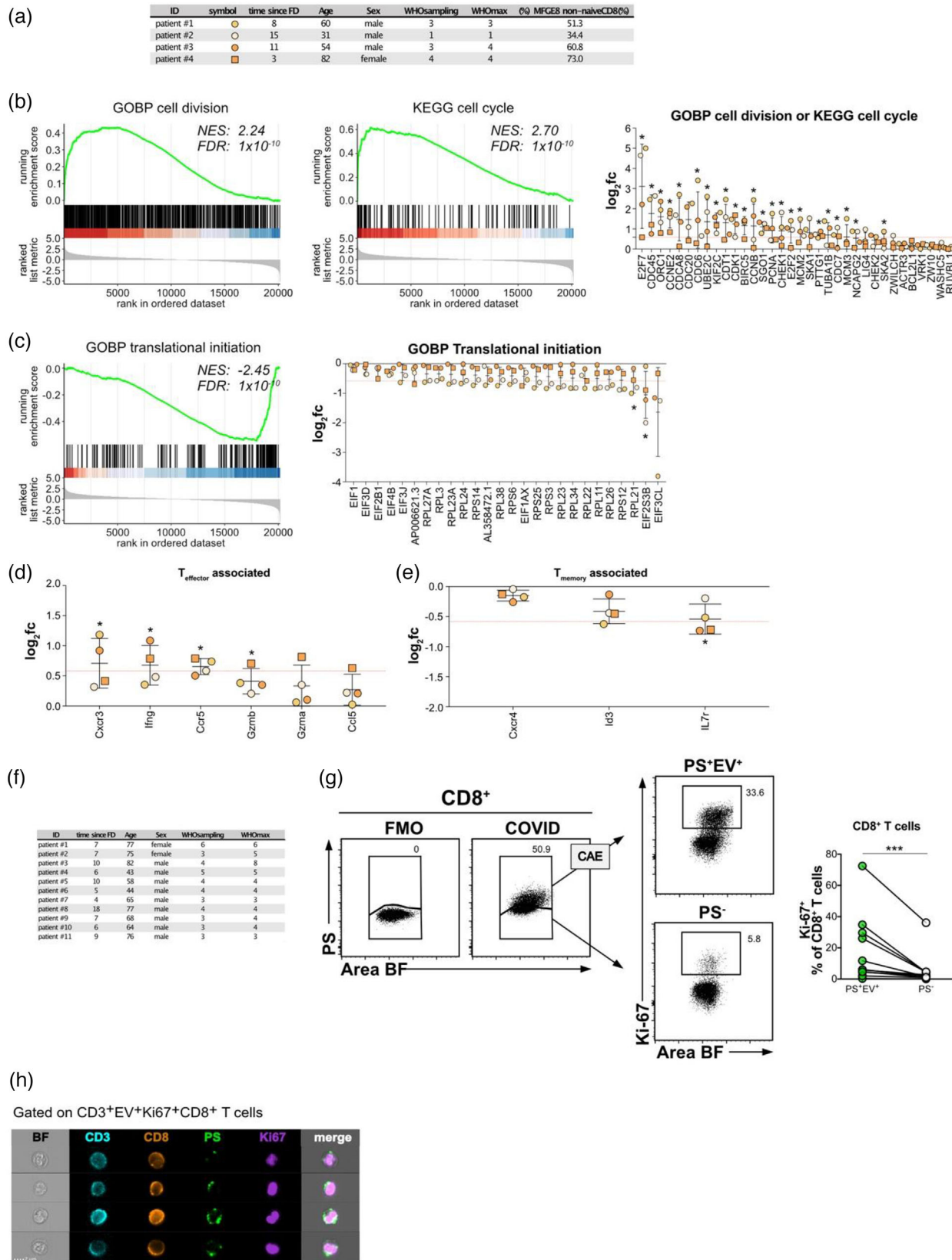


FIGURE 6 PS⁺EV associate with proliferating CD8 T cells. Non-naive PS⁺ and PS⁻ CD8⁺ T cells (gating strategy see Figure S3G) from four patients were sorted and subjected to RNAseq analysis. (a) The table displays patient parameters. (b) GSEA enrichment analysis for the gene sets GOBP cell division and KEGG cell cycle are shown and indicate enrichment in PS⁺ CD8⁺ T cells. Dot plots depict log₂ fold change values of genes in either of these two gene sets and upregulated in all four patients. The red dotted horizontal line indicates a fold change of 1.5 (log₂fc 0.58). *p*-values < 0.05 are indicated with an asterisk. (c) GSEA enrichment analysis for the gene sets GOBP translational initiation and indicates enrichment in PS⁻ CD8⁺ T cells. Dot plots depict log₂ fold change values of genes in this gene set and downregulated in all four patients. The red dotted horizontal line indicates a fold change of -1.5 (log₂fc -0.58).

3 | DISCUSSION

COVID-19 patients have hyperactivated platelets (Zaid et al., 2020), elevated levels of circulating PMPs (Cappellano et al., 2021), and an increased risk of thromboembolic complications contributing to disease severity and mortality. Our results contribute to the complex clinical picture of thromboinflammation (reviewed in Gu et al. (2021) and Lind (2021)). One of our most surprising findings was the high association of PBMC with PS⁺ PMPs and platelets over the disease course, shown with a novel PS-detecting method. The degree of this association correlated more strongly with disease severity than established laboratory indices and might be a promising biomarker for predicting disease severity.

Patients with COVID-19 are mostly lymphopenic (Cao, 2020; Yang et al., 2020), but lymphopenia preferentially affects CD8⁺ T cells (Mathew et al., 2020; Mazzoni et al., 2020). The measurement of dying or apoptotic cells in vivo or fresh ex vivo samples is technically challenging. Phagocytes very efficiently remove dead cells, and sample preparation itself can contribute to cell death. Using novel PS-specific reagents based on lactadherin, we found few but statistically significantly increased amounts of dying PBMCs, but also specifically dying CD8⁺ T cells in the blood of COVID-19 patients.

Antiphospholipid autoantibodies (aPL antibodies), including autoantibodies to the PS/prothrombin complex (antiPS/PT), have been found in COVID-19 patients (Zhang et al., 2020). Hence, it is possible that the association of PS⁺ platelets and PMPs with activated lymphocytes, together with a highly inflammatory environment, may drive the generation of aPL antibodies, further increasing the risk of life-threatening thrombotic events. However, further experiments are necessary to analyse this possibility.

By interacting with the complement cascade activated in COVID-19 patients (Song & FitzGerald, 2020), PS⁺ PMPs could contribute to lymphopenia. Correlation analyses of all blood values with the amounts of PS⁺PMP⁺ PBMCs showed the strongest negative correlation with decreased lymphocyte counts in patients' blood, that is, with established lymphopenia. PS and PS⁺ PMP can activate complement pathways (Mevorach et al., 1998; Tan et al., 2010; Wang et al., 1993), thrombin formation, coagulation and inflammation (Melki et al., 2017; Owens & Mackman, 2011; Ridger et al., 2017). Therefore, one could speculate that PS⁺PMP⁺ T cells might trigger for example the complement cascade on their surface, which might cause cell damage, death and T cell removal by phagocytes.

Moreover, the presence of an activated complement system in COVID-patients (Song & FitzGerald, 2020) could increase the release of PMPs from platelets (Sims et al., 1988) to self-reinforce this spiral. PS⁺ PMPs might facilitate the assembly and dissemination of procoagulant enzyme complexes (Sims et al., 1988). Attracting these reactions to the surface of lymphocytes might cause further functional inhibition or cell death.

'Long Covid' is a phenomenon that occurs in around 10% of COVID-19 patients and seems to be associated with persistent tissue damage in severe cases. However, also patients with mild COVID-19 disease scores might be affected (Mahase, 2020). We identified PS⁺PMP⁺ PBMCs of patients during many weeks post initial diagnosis with only minimal signs of returning to normal levels. Therefore, prolonged adverse effects of PS⁺ PMPs on the immune system could contribute to 'long COVID'. The frequencies of PS⁺ and PS⁺EV⁺ PBMCs in our cohort of recovered patients was only slightly, but statistically significantly elevated when compared to those of healthy donors. As these patients had only mild symptoms (WHO 1–2), it might be interesting to monitor also patients with 'long COVID' or those recovered from severe disease. Eventually PS⁺EV⁺ PBMCs could also be a marker for late COVID-19 symptoms.

Especially CD8⁺ T_{EM} and T_{EMRA} cells, among which most SARS-CoV2-specific clones were identified (Kared et al., 2021) showed enhanced PMP-binding in COVID-19 patients. COVID-19 T cell responses begin too late (Sette & Crotty, 2021), and T cells may be exhausted (Zheng et al., 2020). The association of PS⁺ PMPs with T cells could contribute to these deficiencies and potentially impact the immune and inflammatory antiviral responses. Activated platelets may associate with T cells in the blood of HIV-infected individuals (Green et al., 2015) and link the coagulation and inflammatory cascade with T cells. In vitro, platelets can inhibit proliferation, cytokine production and PD1 expression of T cells (Polasky et al., 2020). Since PMPs derive from platelets, they may also have similar functions as their 'parent'-platelets. We found that between 10% and 80% of CD8⁺ T cells were associated with PD-L1(CD274)⁺ PMP. The fact that we could detect this immunoregulatory molecule on a high frequency of PS⁺ and PS⁻ PMPs raises the possibility that PMPs can suppress CD8⁺ T cells via PD-L1/PD1 interaction. Previous studies suggested that SARS-CoV-2-specific CD8⁺ T cells can have an exhausted phenotype due to their expression of inhibitory receptors such as PD1 (De Biasi et al., 2020; Diao et al., 2020; Song et al., 2020; Zheng et al., 2020). Analogous to PD-L1 on

p-values < 0.05 are indicated with an asterisk. (d and e) Log₂ fold change values of genes associated with T effector (f) and T memory (g) cells that were up- or down-regulated, respectively, in all four patients, are shown. Red dotted horizontal line indicates a fold change of 1.5 (log₂fc 0.58) or -1.5 (log₂fc -0.58).

p-values < 0.05 are indicated with an asterisk. (f) Table shows details of PBMC-origin (patient numbers) for validation experiments shown in (g)-(h). (g) PBMC from COVID patients were examined for proliferation with Ki-67. CD8⁺ T cells (*n* = 11) were analysed as shown in Figure SIF. PS⁺CD3⁺CD8⁺ T cells were stained intranuclear for Ki-67. PS⁺ and PS⁻ fractions were classified by IFC. CAE-analysis identified PS⁺EV⁺ live cells. PS⁺EV⁺ and PS⁻CD8⁺ T cells were then analysed for Ki-67, and data from all patients were plotted on the graph. The numbers in the dot plots represent the fraction of cells in the corresponding gate. Statistical significance was determined by paired Wilcoxon test and is indicated by asterisks (ns *p* > 0.5; **p* ≤ 0.05; ***p* ≤ 0.01; ****p* ≤ 0.001). (h) An image selection of CD8 T cells with the markers used

tumor exosomes, which suppress tumor-specific CD8⁺ T cells (Chen et al., 2018), PD-L1 PMPs could favor T cell suppression in COVID-19. However, recent data have suggested that PD1⁺ SARS-CoV-2-specific CD8⁺ T cells are functional (Rha et al., 2021). Furthermore, our RNAseq results showing subtly increased expression levels of the effector molecules IFN γ , granzyme A, and B and increased proliferation also argue against an exhausted phenotype of PS⁺ CD8⁺ T cells and would instead indicate enhanced effector function or terminal differentiation. Enhanced activation of PS⁺EV⁺ CD8⁺ T cells could theoretically be a reason for the observed higher rate of apoptosis in this population, as activation induced cell death (AICD) is known to contribute to loss of effector T cells (Green et al., 2003).

Two recent studies showed that in COVID-19 patients, hyperactivated platelets could form aggregates with leukocytes and macrophages (Hottz et al., 2020; Manne et al., 2020). As these previous studies relied on conventional flow cytometry, but not IFC, they could not differentiate between CD41⁺ platelets and CD41⁺ PMPs. Also, they did not analyse PS⁺ PMPs on the surface of live lymphocytes. Since PMPs constitute the lion's share of CD41⁺PS⁺ particles on T cells of COVID-19 patients and PS may be responsible for the coagulation and inflammatory effects mentioned above, our findings are an unexpected result with high clinical relevance.

PS is a novel marker to classify COVID-19 patients according to disease severity. Moreover, longitudinal studies could test PS as a predictor of disease development. Due to its ease of use by flow cytometry and the high number of positive PS⁺ PBMC during COVID-19, PS detection could be a valuable analytical tool also in other infectious diseases and sepsis.

4 | MATERIALS AND METHODS

4.1 | Study design and recruitment

Recruited patients ($n = 54$) with PCR confirmed SARS-CoV-2 infection were part of the COVID-19 Registry of the LMU University Hospital Munich (CORKUM, WHO trial id DRKS00021225). The Ethics Committee approved the study of the LMU Munich (No: 20-308; 18-415), and patients included (≥ 18 years, mean age 63, Table S1) consented to serial blood sampling. Additional approval was obtained for the analysis shown here (No. 20-308) and for the use of blood samples from healthy donors (No. 18-415). For this study, patient data were anonymised for analysis, and blood samples were collected between April 2020 and February 2021. Of the 54 patients analysed, 52 patients were hospitalised, and two patients were diagnosed in the hospital and discharged. From 15 patients, blood samples from several timepoints could be obtained, which were taken between days 2 and 76 after a positive SARS-CoV-2 PCR test. Clinical and laboratory data were collected and documented by the CORKUM study group and are summarised in Table S1. We used the World Health Organization's (WHO) eight-point ordinal scale for COVID-19 endpoints (WorldHealthOrganization, 2020) to grade disease severity. WHO scores were combined into 'mild' (WHO 1–3), 'moderate' (WHO 4) and 'severe' (WHO 5–8).

Recovered donors (RD, $n = 12$, mean age 40, Table S1) were adults with a prior SARS-CoV-2 infection (≥ 69 days post positive PCR test), who were either diagnosed in the ambulance or released from the hospital with WHO score 1–2.

Healthy donors (HDs, $n = 35$, mean age 39, Table S1) tested negative for SARS-CoV-2 were used as control cohorts. PBMCs were obtained from leucocyte reduction chambers after thrombocyte donations ($n = 10$) or freshly prepared from whole blood ($n = 25$) of healthy hospital and laboratory workers.

4.2 | Sample processing and cell isolation

Peripheral blood was collected into lithium heparin tubes (Sarstedt) and processed within 6 h after venipuncture. Unfixed samples were handled under Biosafety level 2. PBMCs were isolated by Biocoll density gradient (Merck) centrifugation and then directly stained for imaging flow cytometry.

4.3 | Antibody staining and flow cytometry

Antibodies and staining reagents are listed in Table S2. As PS-staining reagents we used the previously published recombinant MFG-E8-eGFP (Kranich et al., 2020; Trautz et al., 2017) and mCl-biotin multimerised with streptavidin-AF647 for flow cytometry or streptavidin-gold for TEM. mCl-multimers are commercially available through BioLegend as ApotrackerTM Tetra reagents. In flow cytometry. All PS-staining reagents are Ca²⁺ independent, highly stable and PS-specific. Freshly isolated PBMCs were incubated with Fc block before live/dead and cell surface antibody staining. PBMCs surface staining was performed in staining buffer (PBS containing 2% of fetal calf serum) for 25 min on ice. Then cells were washed and fixed with 4% PFA for 30 min at room temperature (RT), washed again, filtered and analysed on an ImageStreamx MKII imaging flow cytometer (Luminex). Samples

were acquired with low flow rate/high sensitivity and 60× magnification. Images were acquired using bright field illumination and the excitation lasers 405, 488, 561 and 642 nm.

For intranuclear Ki-67 staining, cells were fixed and permeabilised using the Transcription Factor Staining Buffer Set (ThermoFisher, cat. #00-5523-00) according to the manufacturers' instructions. Intranuclear staining was performed in permeabilisation buffer for 30 min at RT.

4.4 | Cell sorting for gene expression analysis

PBMCs from four patients (see Figure 6a) were stained with anti-CD3-BV421, anti-CD8-BV785, anti-CCR7-APC, anti-CD45RA-PerCPCy5.5, anti-CD19/CD16/CD56/CD14-APCFire750 and MFG-E8-eGFP (see Table S2) in staining buffer (25 min, 4°C) after cells were incubated with Fixable Viability dye eFluor780 in PBS (10 min, 4°C). PS⁺ and PS⁻ single, live, non-naïve (CCR7⁺CD45RA⁻, CCR7⁻CD45RA⁻ and CCR7⁻CD45RA⁺) CD3⁺CD8⁺ T cells were directly sorted into TRIzol reagent (Thermo Fisher) on a FACS Aria Fusion (BD) using a 100 μm nozzle. Samples were stored at -20°C until analysis. RNA isolation and sequencing were performed by Vertis Biotechnologie AG, Freising. Total RNA was isolated and purified using Monarch columns (NEB). Poly(A)⁺ RNA was isolated from the total RNA sample. First-strand cDNA synthesis was primed with a N6 randomised primer. After fragmentation, the Illumina TruSeq sequencing adapters were ligated in a strand specific manner to the 5' and 3' ends of the cDNA fragments. In this way, a strand specific PCR amplification of the cDNA was achieved using a proof-reading enzyme. For Illumina NextSeq sequencing, the samples were pooled in approximately equimolar amounts. The cDNA pool in the size range of 250–700 bp was eluted from a preparative agarose gel. The primers used for PCR amplification were designed for TruSeq sequencing according to the instructions of Illumina. The cDNA size range was 250–700 bp. The cDNA pool was sequenced on an Illumina NextSeq 500 system using 1 × 75 bp read length.

4.5 | RNAseq analysis

Sequencing reads were aligned to the human reference genome (version GRCH38.100) with STAR (version 2.7.3). Expression values (TPM) were calculated with RSEM (version 1.3.3). Post-processing was performed in R/bioconductor (version 4.0.3) using default parameters if not indicated otherwise. Differential gene expression analysis was performed with 'DEseq2' (version 1.28.1) using a model including patient ID as random factor. An adjusted *p* value (FDR) of less than 0.1 was used to classify significantly changed expression. Gene set enrichment analyses were conducted with 'clusterProfiler' (version 3.18.1) on the statistic reported by DEseq2. Data are available at GEO Submission (GSE174786).

4.6 | Cell sorting for TEM

Isolated PBMCs were stained with anti-CD19- and anti-CD3-PE, PS-staining reagent mC1-multimer (SA-AF647) (commercially available at BioLegend) and mC1-biotin (commercially available at BioLegend) multimerised with SA-gold, (Aurion) (see Table S2) in staining buffer (25 min, 4°C) after incubation with Fixable Viability Dye eFluor780 in PBS (10 min, 4°C). After washing, cells were prefixed with freshly prepared 4% EM-grade PFA (Science Services) for 30 min at RT before sorting. Fixed, single, PS⁺CD19⁺ and CD3⁺ cells were sorted on a FACS Aria III (BDBiosciences) using a 130 μm nozzle into PBS containing 0.5% BSA.

After washing with PBS, cells were fixed with 2.5% glutaraldehyde (EM-grade, Science Services) in 0.1 M cacodylate buffer (pH 7.4) for 15 min (Sigma Aldrich) and washed with 0.1 M sodium cacodylate buffer for 10 min at 400 g before postfixation in reduced osmium (1% osmium tetroxide (Science Services), 0.8% potassium ferricyanide (Sigma Aldrich) in 0.1 M sodium cacodylate buffer). The cell pellet was contrasted in 0.5% uranyl acetate in water (Science Services) and dehydrated in an ascending ethanol series. The pellet was embedded in epon resin and hardened for 48 h at 60°C. Ultra-thin sections (50 nm) were cut and deposited onto formvar-coated grids (Plano) and again contrasted using 1% uranyl acetate in water and Ultrastain (Leica). Images were acquired on a JEM 1400plus (JEOL).

4.7 | Imaging flow cytometry and data analysis

Data analysis was performed using the IDEAS software (Version 6.2, Luminex). Compensation matrices were generated using single stained samples and applied to the raw data, and data analysis files were created. Unfocused events were excluded from the analysis based on gradient max feature values. PS⁺ cells were gating using FMO controls. TIFF-images of PS⁺ cells from each sample were exported (16-bit, raw) and analysed by the CAE algorithm as previously described (Kranich et al., 2020). Two *.pop

files containing the object numbers of apoptotic and EV⁺ cells were generated and re-imported into the IDEAS software. Then FCS files from all cells, only apoptotic or only EV⁺ cells, were exported and analysed using FlowJo Version 10.7.1.

4.8 | Colocalisation analysis

We created a spot mask for PS and the respective marker staining to determine the degree of colocalisation between PS⁺ EVs and PMP-marker⁺ (CD41/CD63/CD274/CD62P) cells. PS⁺ spots were identified by the Dilate (Peak(M02, PS, Bright, 5),1) mask and the Dilate(Peak(M_marker, marker channel, Bright, 1),1) mask was used to identify marker⁺ spots. Both masks were combined, and the colocalisation was assessed using the BDS R3 feature of the IDEAS software.

4.9 | Platelet staining

Platelets were stained in whole blood. Hundred microlitres of blood were slowly added to 100 μ l of antibody mix in staining buffer (PBS with 0.1% sodium azide and 2% of FCS). The mixture was gently swirled and incubated for 30 min at room temperature in the dark. Then cells were fixed in 1% PFA in PBS with 0.1% sodium azide for 2 h, centrifuged for 20 min at 5000 g, resuspended in PBS with 0.1% sodium azide and analysed on the ImageStreamx MKII imaging flow cytometer.

4.10 | Statistical analysis

For statistical analysis, the PRISM software (GraphPad Software, La Jolla, CA, USA) was used. For direct comparison between two groups non-parametric, unpaired Mann-Whitney test was used. Statistical significance of paired data was determined by paired Wilcoxon test. p values of ≤ 0.05 are considered significant and denoted with *, ** $p < 0.01$, *** $p < 0.001$ and **** $p < 0.0001$. R version 4.0.3 was used for correlation analysis. Numeric values in the dataset were correlated (Spearman correlation) using the ggcorrmat function of the ggstatsplot package (v0.7.2) with Benjamini-Hochberg correction for multiple testing.

ROC analysis was performed using library 'pROC' (version 1.17.01). Thresholds were determined using the pROCs coords function with the 'best' method.

ACKNOWLEDGEMENTS

We would like to thank all of the COVID-19 Registry of the LMU Munich (CORKUM) investigators and staff and the patients and their families for participating in the CORKUM registry and all health care workers for their outstanding service. We acknowledge the Core Facility Flow Cytometry at the Biomedical Center, LMU Munich, for providing the ImageStreamX MKII imaging flow cytometer, cell sorters and services. We thank Wenbo Hu for providing reagents. T.B. and A.K. are supported by the Deutsche Forschungsgemeinschaft under CRC 1054 (TP B03, grant no. 210592381; and TP A06, grant no. 210592381). A.K. received funding from Deutsche Forschungsgemeinschaft under CRC/TR237-B14 (369799452) and KR2199/10-1 (391217598), and received funding from the Bavarian State Ministry of Science and the Arts.

CONFLICT OF INTERESTS

T.B. and J.K. declare competing interests due an exclusive licensing agreement with BioLegend, Inc. for the commercialisation of mCI-multimer. The remaining authors declare no competing interests.

AUTHOR CONTRIBUTIONS

Lisa Rausch: Formal analysis; Investigation; writing original draft. Konstantin Lutz: Formal analysis. Martina Schifferer: Formal analysis; Investigation; Writing – review & editing. Elena Winheim: Resources. Rudi Gruber: Investigation Formal analysis; Writing – review & editing. Anne B. Krug: Writing – review & editing, supervision, funding acquisition. Linus Rinke: Investigation. Clemens Scherer: Resources. Johannes C. Hellmuth: Resources. Maximilian Muenchhoff: Resources; Writing – review & editing. Christopher Mandel: Resources. Michael Bergwelt: Resources. Mikael Simons: Formal analysis; Funding acquisition; Writing – review & editing. Tobias Straub: Formal analysis. Jan Kranich: Conceptualization; Investigation; Software; Writing – original draft; Supervision. Thomas Brocker: Conceptualization; Funding acquisition; Supervision; Writing – original draft.

ORCID

Jan Kranich  <https://orcid.org/0000-0002-9928-4132>

Thomas Brocker  <https://orcid.org/0000-0001-7060-5433>

REFERENCES

- Aatonen, M. T., Ohman, T., Nyman, T. A., Laitinen, S., Grönholm, M., & Siljander, P. R. (2014). Isolation and characterization of platelet-derived extracellular vesicles. *Journal of Extracellular Vesicles*, 3(1), 24692, <https://doi.org/10.3402/jev.v3.24692>.
- Arraud, N., Linares, R., Tan, S., Gounou, C., Pasquet, J. M., Mornet, S., & Brisson, A. R. (2014). Extracellular vesicles from blood plasma: Determination of their morphology, size, phenotype and concentration. *Journal of Thrombosis and Haemostasis*, 12, 614–627, <https://doi.org/10.1111/jth.12554>.
- Best, J. A., Blair, D. A., Knell, J., Yang, E., Mayya, V., Doedens, A., Dustin, M. L., Goldrath, A. W., & Immunological Genome Project Consortium (2013). Transcriptional insights into the CD8+ T cell response to infection and memory T cell formation. *Nature Immunology*, 14, 404–412, <https://doi.org/10.1038/ni.2536>.
- Braun, J., Loyal, L., Frentsch, M., Wendisch, D., Georg, P., Kurth, F., Hippenstiel, S., Dingeldey, M., Kruse, B., Fauchere, F., Baysal, E., Mangold, M., Henze, L., Lauster, R., Mall, M. A., Beyer, K., Röhmel, J., Voigt, S., Schmitz, J., ... Thiel, A. (2020). SARS-CoV-2-reactive T cells in healthy donors and patients with COVID-19. *Nature*, 587, 270–274, <https://doi.org/10.1038/s41586-020-2598-9>.
- Cao, X. (2020). COVID-19: Immunopathology and its implications for therapy. *Nature Reviews Immunology*, 20, 269–270, <https://doi.org/10.1038/s41577-020-0308-3>.
- Cappellano, G., Raineri, D., Rolla, R., Giordano, M., Puricelli, C., Vilardo, B., Manfredi, M., Cantaluppi, V., Sainaghi, P. P., Castello, L., De Vita, N., Scotti, L., Vaschetto, R., Dianzani, U., & Chiochetti, A. (2021). Circulating platelet-derived extracellular vesicles are a hallmark of Sars-Cov-2 infection. *Cells* 10, 85, <https://doi.org/10.3390/cells10010085>.
- Chapman, L. M., Aggrey, A. A., Field, D. J., Srivastava, K., Ture, S., Yui, K., Topham, D. J., Baldwin, W. M. 3rd, & Morrell, C. N. (2012). Platelets present antigen in the context of MHC class I. *Journal of Immunology*, 189, 916–923, <https://doi.org/10.4049/jimmunol.1200580>.
- Chen, G., Huang, A. C., Zhang, W., Zhang, G., Wu, M., Xu, W., Yu, Z., Yang, J., Wang, B., Sun, H., Xia, H., Man, Q., Zhong, W., Antelo, L. F., Wu, B., Xiong, X., Liu, X., Guan, L., Li, T., ... Guo, W. (2018). Exosomal PD-L1 contributes to immunosuppression and is associated with anti-PD-1 response. *Nature*, 560, 382–386, <https://doi.org/10.1038/s41586-018-0392-8>.
- Chen, R., Sang, L., Jiang, M., Yang, Z., Jia, N., Fu, W., Xie, J., Guan, W., Liang, W., Ni, Z., Hu, Y., Liu, L., Shan, H., Lei, C., Peng, Y., Wei, L., Liu, Y., Hu, Y., Peng, P., ... Medical Treatment Expert Group for COVID-19 (2020). Longitudinal hematologic and immunologic variations associated with the progression of COVID-19 patients in China. *Journal of Allergy and Clinical Immunology*, 146, 89–100, <https://doi.org/10.1016/j.jaci.2020.05.003>.
- Connor, D. E., Exner, T. M., Da, D., & Joseph, J. E. (2010). The majority of circulating platelet-derived microparticles fail to bind annexin V, lack phospholipid-dependent procoagulant activity and demonstrate greater expression of glycoprotein Ib. *Thrombosis and Haemostasis*, 103, 1044–1052, <https://doi.org/10.1160/TH09-09-0644>.
- Corban, M. T., Duarte-Garcia, A., McBane, R. D., Matteson, E. L., Lerman, L. O., & Lerman, A. (2017). Antiphospholipid syndrome: Role of vascular endothelial cells and implications for risk stratification and targeted therapeutics. *Journal of the American College of Cardiology*, 69, 2317–2330, <https://doi.org/10.1016/j.jacc.2017.02.058>.
- De Biasi, S., Meschieri, M., Gibellini, L., Bellinazzi, C., Borella, R., Fidanza, L., Gozzi, L., Iannone, A., Lo Tartaro, D., Mattioli, M., Paolini, A., Menozzi, M., Milić, J., Franceschi, G., Fantini, R., Tonelli, R., Sita, M., Sarti, M., Trenti, T., ... Cossarizza, A. (2020). Marked T cell activation, senescence, exhaustion and skewing towards TH17 in patients with COVID-19 pneumonia. *Nature Communications*, 11, 3434, <https://doi.org/10.1038/s41467-020-17292-4>.
- DeGregori, J., & Johnson, D. G. (2006). Distinct and overlapping roles for E2F family members in transcription, proliferation and apoptosis. *Current Molecular Medicine*, 6, 739–748, <https://doi.org/10.2174/1566524010606070739>.
- Del Valle, D. M., Kim-Schulze, S., Huang, H. H., Beckmann, N. D., Nirenberg, S., Wang, B., Lavin, Y., Swartz, T. H., Madduri, D., Stock, A., Marron, T. U., Xie, H., Patel, M., Tuballes, K., Van Oekelen, O., Rahman, A., Kovatch, P., Aberg, J. A., Schadt, E., ... Gnjatich, S. (2020). An inflammatory cytokine signature predicts COVID-19 severity and survival. *Nature Medicine*, 26, 1636–1643, <https://doi.org/10.1038/s41591-020-1051-9>.
- Diao, B., Wang, C., Tan, Y., Chen, X., Liu, Y., Ning, L., Chen, L., Li, M., Liu, Y., Wang, G., Yuan, Z., Feng, Z., Zhang, Y., Wu, Y., & Chen, Y. (2020). Reduction and functional exhaustion of T cells in patients with coronavirus disease 2019 (COVID-19). *Frontiers in Immunology*, 11, 827, <https://doi.org/10.3389/fimmu.2020.00827>.
- Green, D. R., Droin, N., & Pinkoski, M. (2003). Activation-induced cell death in T cells. *Immunological Reviews*, 193, 70–81, <https://doi.org/10.1034/j.1600-065x.2003.00051.x>.
- Green, S. A., Smith, M., Hasley, R. B., Stephany, D., Harned, A., Nagashima, K., Abdullah, S., Pittaluga, S., Imamichi, T., Qin, J., Rupert, A., Ober, A., Lane, H. C., & Catalfamo, M. (2015). Activated platelet-T-cell conjugates in peripheral blood of patients with HIV infection: coupling coagulation/inflammation and T cells. *Aids*, 29, 1297–1308, <https://doi.org/10.1097/QAD.0000000000000701>.
- Gu, S. X., Tyagi, T., Jain, K., Gu, V. W., Lee, S. H., Hwa, J. M., Kwan, J. M., Krause, D. S., Lee, A. I., Halene, S., Martin, K. A., Chun, H. J., & Hwa, J. (2021). Thrombocytopeny and endotheliopathy: crucial contributors to COVID-19 thromboinflammation. *Nature Reviews Cardiology*, 18, 194–209, <https://doi.org/10.1038/s41569-020-00469-1>.
- Guan, W. J., Ni, Z. Y., Hu, Y., Liang, W. H., Ou, C. Q., He, J. X., Liu, L., Shan, H., Lei, C. L., Hui, D. S. C., Du, B., Li, L. J., Zeng, G., Yuen, K. Y., Chen, R. C., Tang, C. L., Wang, T., Chen, P. Y., Xiang, J., ... China Medical Treatment Expert Group for Covid-19. (2020) Clinical Characteristics of Coronavirus Disease 2019 in China. *New England Journal of Medicine*, 382, 1708–1720, <https://doi.org/10.1056/NEJMoa2002032>.
- Heijnen, H. F., Schiel, A. E., Fijnheer, R., Geuze, H. J., & Sixma, J. J. (1999). Activated platelets release two types of membrane vesicles: microvesicles by surface shedding and exosomes derived from exocytosis of multivesicular bodies and alpha-granules. *Blood*, 94, 3791–3799.
- Hotchkiss, R. S., & Nicholson, D. W. (2006). Apoptosis and caspases regulate death and inflammation in sepsis. *Nature Reviews Immunology*, 6, 813–822, <https://doi.org/10.1038/nri1943>.
- Hottz, E. D., Azevedo-Quintanilha, I. G., Palhinha, L., Teixeira, L., Barreto, E. A., Pão, C. R. R., Righy, C., Franco, S., Souza, T. M. L., Kurtz, P., Bozza, F. A., & Bozza, P. T. (2020). Platelet activation and platelet-monocyte aggregate formation trigger tissue factor expression in patients with severe COVID-19. *Blood*, 136, 1330–1341, <https://doi.org/10.1182/blood.2020007252>.
- Huang, C., Wang, Y., Li, X., Ren, L., Zhao, J., Hu, Y., Zhang, L., Fan, G., Xu, J., Gu, X., Cheng, Z., Yu, T., Xia, J., Wei, Y., Wu, W., Xie, X., Yin, W., Li, H., Liu, M., ... Cao, B. (2020). Clinical features of patients infected with 2019 novel coronavirus in Wuhan, China. *Lancet*, 395, 497–506, [https://doi.org/10.1016/S0140-6736\(20\)30183-5](https://doi.org/10.1016/S0140-6736(20)30183-5).
- Huang, T. M., Ishida, T., Harashima, H., & Kiwada, H. (2001). The complement system enhances the clearance of phosphatidylserine (PS)-liposomes in rat and guinea pig. *International Journal of Pharmaceutics*, 215, 197–205, [https://doi.org/10.1016/s0378-5173\(00\)00691-8](https://doi.org/10.1016/s0378-5173(00)00691-8).
- Kared, H., Redd, A. D., Bloch, E. M., Bonny, T. S., Sumatoh, H., Kairi, F., Carbajo, D., Abel, B., Newell, E. W., Bettinotti, M. P., Benner, S. E., Patel, E. U., Littlefield, K., Laeyendecker, O., Shoham, S., Sullivan, D., Casadevall, A., Pekosz, A., Nardin, A., ... Quinn, T. C. (2021). SARS-CoV-2-specific CD8+ T cell responses in convalescent COVID-19 individuals. *Journal of Clinical Investigation*, 131, e145476, <https://doi.org/10.1172/JCI145476>.

- Klok, F. A., Kruij, M. J. H. A., van der Meer, N. J. M., Arbous, M. S., Gommers, D. A. M. P. J., Kant, K. M., Kaptein, F. H. J., van Paassen, J., Stals, M. A. M., Huisman, M. V., & Endeman, H. (2020). Incidence of thrombotic complications in critically ill ICU patients with COVID-19. *Thrombosis Research*, *191*, 145–147, <https://doi.org/10.1016/j.thromres.2020.04.013>.
- Kranich, J., Chlis, N. K., Rausch, L., Latha, A., Schifferer, M., Kurz, T., Foltyn-Arfa Kia, A., Simons, M., Theis, F. J., & Brocker, T. (2020). In vivo identification of apoptotic and extracellular vesicle-bound live cells using image-based deep learning. *Journal of Extracellular Vesicles*, *9*, 1792683, <https://doi.org/10.1080/20013078.2020.1792683>.
- Laing, A. G., Lorenc, A., Del Molino Del Barrio, I., Das, A., Fish, M., Monin, L., Muñoz-Ruiz, M., McKenzie, D. R., Hayday, T. S., Francos-Quijorna, I., Kamdar, S., Joseph, M., Davies, D., Davis, R., Jennings, A., Zlatareva, I., Vantourout, P., Wu, Y., Sofra, V., ... Hayday, A. C. (2020). A dynamic COVID-19 immune signature includes associations with poor prognosis. *Nature Medicine*, *26*, 1623–1635, <https://doi.org/10.1038/s41591-020-1038-6>.
- Li, Q., Ding, X., Xia, G., Chen, H. G., Chen, F., Geng, Z., Xu, L., Lei, S., Pan, A., Wang, L., & Wang, Z. (2020). Eosinopenia and elevated C-reactive protein facilitate triage of COVID-19 patients in fever clinic: A retrospective case-control study. *EclinicalMedicine*, *23*, 100375, <https://doi.org/10.1016/j.eclinm.2020.100375>.
- Liao, M., Liu, Y., Yuan, J., Wen, Y., Xu, G., Zhao, J., Cheng, L., Li, J., Wang, X., Wang, F., Liu, L., Amit, I., Zhang, S., & Zhang, Z. (2020). Single-cell landscape of bronchoalveolar immune cells in patients with COVID-19. *Nature Medicine*, *26*, 842–844, <https://doi.org/10.1038/s41591-020-0901-9>.
- Lind, S. E. (2021). Phosphatidylserine is an overlooked mediator of COVID-19 thromboinflammation. *Heliyon*, *7*, e06033, <https://doi.org/10.1016/j.heliyon.2021.e06033>.
- Lippi, G., & Plebani, M. (2020). Laboratory abnormalities in patients with COVID-2019 infection. *Clinical Chemistry and Laboratory Medicine*, *58*, 1131–1134, <https://doi.org/10.1515/cclm-2020-0198>.
- Liu, J., Li, S., Liu, J., Liang, B., Wang, X., Wang, H., Li, W., Tong, Q., Yi, J., Zhao, L., Xiong, L., Guo, C., Tian, J., Luo, J., Yao, J., Pang, R., Shen, H., Peng, C., Liu, T., ... Zheng, X. (2020). Longitudinal characteristics of lymphocyte responses and cytokine profiles in the peripheral blood of SARS-CoV-2 infected patients. *EBioMedicine*, *55*, 102763, <https://doi.org/10.1016/j.ebiom.2020.102763>.
- MacLaren, G., Fisher, D., & Brodie, D. (2020). Preparing for the most critically ill patients with COVID-19: The potential role of extracorporeal membrane oxygenation. *Jama*, *323*, 1245–1246, <https://doi.org/10.1001/jama.2020.2342>.
- Mahase, E. (2020). Long covid could be four different syndromes, review suggests. *Bmj (Clinical Research Ed.)*, *371*, m3981, <https://doi.org/10.1136/bmj.m3981>.
- Manne, B. K., Denorme, F., Middleton, E. A., Portier, I., Rowley, J. W., Stubben, C., Petrey, A. C., Tolley, N. D., Guo, L., Cody, M., Weyrich, A. S., Yost, C. C., Rondina, M. T., & Campbell, R. A. (2020). Platelet gene expression and function in patients with COVID-19. *Blood*, *136*, 1317–1329, <https://doi.org/10.1182/blood.2020007214>.
- Mathew, D., Giles, J. R., Baxter, A. E., Oldridge, D. A., Greenplate, A. R., Wu, J. E., Alanio, C., Kuri-Cervantes, L., Pampena, M. B., D'Andrea, K., Manne, S., Chen, Z., Huang, Y. J., Reilly, J. P., Weisman, A. R., Ittner, C. A. G., Kuthuru, O., Dougherty, J., Nzingha, K., ... Wherry, E. J. (2020). Deep immune profiling of COVID-19 patients reveals distinct immunotypes with therapeutic implications. *Science*, *369*, eabc8511, <https://doi.org/10.1126/science.abc8511>.
- Mathieu, M., Martin Jaular, L., Lavieue, G., & Théry, C. (2018). Specificities of secretion and uptake of exosomes and other extracellular vesicles for cell-to-cell communication. *Nature Cell Biology*, *21*, 1–9, <https://doi.org/10.1038/s41556-018-0250-9>.
- Mazzoni, A., Salvati, L., Maggi, L., Capone, M., Vanni, A., Spinicci, M., Mencarini, J., Caporale, R., Peruzzi, B., Antonelli, A., Trotta, M., Zammarchi, L., Ciani, L., Gori, L., Lazzeri, C., Matucci, A., Vultaggio, A., Rossi, O., Almerigogna, F., ... Cosmi, L. (2020). Impaired immune cell cytotoxicity in severe COVID-19 is IL-6 dependent. *Journal of Clinical Investigation*, *130*, 4694–4703, <https://doi.org/10.1172/JCI138554>.
- Melki, I., Tessandier, N., Zufferey, A., & Boilard, E. (2017). Platelet microvesicles in health and disease. *Platelets*, *28*, 214–221, <https://doi.org/10.1080/09537104.2016.1265924>.
- Mevorach, D., Mascarenhas, J. O., Gershov, D., & Elkon, K. B. (1998). Complement-dependent clearance of apoptotic cells by human macrophages. *Journal of Experimental Medicine*, *188*, 2313–2320, <https://doi.org/10.1084/jem.188.12.2313>.
- Middeldorp, S., Coppens, M., van Haaps, T. F., Foppen, M., Vlaar, A. P., Müller, M. C. A., Bouman, C. C. S., Beenen, L. F. M., Kootte, R. S., Heijmans, J., Smits, L. P., Bonta, P. I., & van Es, N. (2020). Incidence of venous thromboembolism in hospitalized patients with COVID-19. *Journal of Thrombosis and Haemostasis*, *18*, 1995–2002, <https://doi.org/10.1111/jth.14888>.
- Owens, A. P. 3rd, & Mackman, N. (2011). Microparticles in hemostasis and thrombosis. *Circulation Research*, *108*, 1284–1297, <https://doi.org/10.1161/CIRCRESAHA.110.233056>.
- Paidassi, H., Tacnet-Delorme, P., Garlatti, V., Darnault, C., Ghebrehiwet, B., Gaboriaud, C., Arlaud, G. J., & Frachet, P. (2008). CIq binds phosphatidylserine and likely acts as a multiligand-bridging molecule in apoptotic cell recognition. *Journal of Immunology*, *180*, 2329–2338.
- Polasky, C., Wendt, F., Pries, R., & Wollenberg, B. (2020). Platelet induced functional alteration of CD4(+) and CD8(+) T cells in HNSCC. *International Journal of Molecular Sciences*, *21*, 7507, <https://doi.org/10.3390/ijms21207507>.
- Ponomareva, A. A., Nevzorova, T. A., Mordakhanova, E. R., Andrianova, I. A., Rauova, L., Litvinov, R. I., & Weisel, J. W. (2017). Intracellular origin and ultrastructure of platelet-derived microparticles. *Journal of Thrombosis and Haemostasis*, *15*, 1655–1667, <https://doi.org/10.1111/jth.13745>.
- Reininger, A. J., Heijnen, H. F., Schumann, H., Specht, H. M., Schramm, W., & Ruggeri, Z. M. (2006). Mechanism of platelet adhesion to von Willebrand factor and microparticle formation under high shear stress. *Blood*, *107*, 3537–3545, <https://doi.org/10.1182/blood-2005-02-0618>.
- Rha, M. S., Jeong, H. W., Ko, J. H., Choi, S. J., Seo, I. H., Lee, J. S., Sa, M., Kim, A. R., Joo, E. J., Ahn, J. Y., Kim, J. H., Song, K. H., Kim, E. S., Oh, D. H., Ahn, M. Y., Choi, H. K., Jeon, J. H., Choi, J. P., Kim, H. B., ... Shin, E. C. (2021). PD-1-Expressing SARS-CoV-2-Specific CD8(+) T Cells Are Not Exhausted, but Functional in Patients with COVID-19. *Immunity*, *54*, 44–52 e43, <https://doi.org/10.1016/j.immuni.2020.12.002>.
- Ridger, V. C., Boulanger, C. M., Angelillo-Scherrer, A., Badimon, L., Blanc-Brude, O., Bochaton-Piallat, M. L., Boilard, E., Buzas, E. I., Caporali, A., Dignat-George, F., Evans, P. C., Lacroix, R., Lutgens, E., Ketelhuth, D. F. J., Nieuwland, R., Toti, F., Tunon, J., Weber, C., & Hofer, I. E. (2017). Microvesicles in vascular homeostasis and diseases. Position Paper of the European Society of Cardiology (ESC) Working Group on Atherosclerosis and Vascular Biology. *Thrombosis and Haemostasis*, *117*, 1296–1316, <https://doi.org/10.1160/TH16-12-0943>.
- Rolfes, V., Idel, C., Pries, R., Plötze-Martin, K., Habermann, J., Gemoll, T., Bohnet, S., Latz, E., Ribbat-Idel, J., Franklin, B. S., & Wollenberg, B. (2018). PD-L1 is expressed on human platelets and is affected by immune checkpoint therapy. *Oncotarget*, *9*, 27460–27470, <https://doi.org/10.18632/oncotarget.25446>.
- Rydzynski Moderbacher, C., Ramirez, S. I., Dan, J. M., Grifoni, A., Hastie, K. M., Weiskopf, D., Belanger, S., Abbott, R. K., Kim, C., Choi, J., Kato, Y., Crotty, E. G., Kim, C., Rawlings, S. A., Mateus, J., Tse, L. P. V., Frazier, A., Baric, R., Peters, B., ... Crotty, S. (2020). Antigen-Specific Adaptive Immunity to SARS-CoV-2 in Acute COVID-19 and Associations with Age and Disease Severity. *Cell*, *183*, 996–1012 e1019, <https://doi.org/10.1016/j.cell.2020.09.038>.
- Sachs, A. B. (2000). Cell cycle-dependent translation initiation: IRES elements prevail. *Cell*, *101*, 243–245, [https://doi.org/10.1016/s0092-8674\(00\)80834-x](https://doi.org/10.1016/s0092-8674(00)80834-x).
- Sallusto, F., Geginat, J., & Lanzavecchia, A. (2004). Central memory and effector memory T cell subsets: Function, generation, and maintenance. *Annual Review of Immunology*, *22*, 745–763, <https://doi.org/10.1146/annurev.immunol.22.012703.104702>.
- Scholzen, T., & Gerdes, J. (2000). The Ki-67 protein: From the known and the unknown. *Journal of Cellular Physiology*, *182*, 311–322, [https://doi.org/10.1002/\(sici\)1097-4652\(200003\)182:3<311::Aid-jcp1>3.0.Co;2-9](https://doi.org/10.1002/(sici)1097-4652(200003)182:3<311::Aid-jcp1>3.0.Co;2-9).

- Sekine, T., Perez-Potti, A., Rivera-Ballesteros, O., Strålin, K., Gorin J. B., Olsson A., Llewellyn-Lacey, S., Kamal, H., Bogdanovic, G., Muschiol S., Wullmann D. J., Kammann, T., Emgård, J., Parrot, T., Folkesson, E., Karolinska COVID-19 Study Group, Rooyackers, O., Eriksson, L. I., Henter, J. I., ... Buggert, M. (2020). Robust T cell immunity in convalescent individuals with asymptomatic or mild COVID-19. *Cell* 183, 158–168 e114, <https://doi.org/10.1016/j.cell.2020.08.017>.
- Sette, A., & Crotty, S. (2021). Adaptive immunity to SARS-CoV-2 and COVID-19. *Cell*, 184, 861–880, <https://doi.org/10.1016/j.cell.2021.01.007>.
- Sims, P. J., Faioni, E. M., Wiedmer, T., & Shattil, S. J. (1988). Complement proteins C5b-9 cause release of membrane vesicles from the platelet surface that are enriched in the membrane receptor for coagulation factor Va and express prothrombinase activity. *Journal of Biological Chemistry*, 263, 18205–18212.
- Song, J. W., Zhang, C., Fan, X., Meng, F. P., Xu, Z., Xia, P., Cao, W. J., Yang, T., Dai, X. P., Wang, S. Y., Xu, R. N., Jiang, T. J., Li, W. G., Zhang, D. W., Zhao, P., Shi, M., Agrati, C., Ippolito, G., Maeurer, M., ... Zhang, J. Y. (2020). Immunological and inflammatory profiles in mild and severe cases of COVID-19. *Nature Communications*, 11, 3410, <https://doi.org/10.1038/s41467-020-17240-2>.
- Song, J., So, T., Cheng, M., Tang, X., & Croft, M. (2005). Sustained survivin expression from OX40 costimulatory signals drives T cell clonal expansion. *Immunity*, 22, 621–631, <https://doi.org/10.1016/j.immuni.2005.03.012>.
- Song, W. C., & FitzGerald, G. A. (2020). COVID-19, microangiopathy, hemostatic activation, and complement. *Journal of Clinical Investigation*, 130, 3950–3953, <https://doi.org/10.1172/JCI140183>.
- Su, Y., Chen, D., Yuan, D., Lausted, C., Choi, J., Dai, C. L., Voillet, V., Duvvuri, V. R., Scherler, K., Troisch, P., Baloni, P., Qin, G., Smith, B., Kornilov, S. A., Rostomily, C., Xu, A., Li, J., Dong, S., Rothchild, A., ... Heath, J. R. (2020). Multi-omics resolves a sharp disease-state shift between mild and moderate COVID-19. *Cell*, 183, 1479–1495 e1420, <https://doi.org/10.1016/j.cell.2020.10.037>.
- Tan, A. T., Linster, M., Tan, C. W., Le Bert, N., Chia, W. N., Kunasegaran, K., Zhuang, Y., Tham, C. Y. L., Chia, A., Smith, G. J. D., Young, B., Kalimuddin, S., Low, J. G. H., Lye, D., Wang, L. F., & Bertoletti, A. (2021). Early induction of functional SARS-CoV-2-specific T cells associates with rapid viral clearance and mild disease in COVID-19 patients. *Cell Reports*, 34(6), 108728, <http://doi.org/10.1016/j.celrep.2021.108728>.
- Tan, L. A., Yu, B., Sim, F. C., Kishore, U., & Sim, R. B. (2010). Complement activation by phospholipids: The interplay of factor H and Clq. *Protein Cell*, 1, 1033–1049, <https://doi.org/10.1007/s13238-010-0125-8>.
- Tang, N., Li, D., Wang, X., & Sun, Z. (2020). Abnormal coagulation parameters are associated with poor prognosis in patients with novel coronavirus pneumonia. *Journal of Thrombosis and Haemostasis*, 18, 844–847, <https://doi.org/10.1111/jth.14768>.
- Teuwen, L. A., Geldhof, V., Pasut, A., & Carmeliet, P. (2020). COVID-19: the vasculature unleashed. *Nature Reviews Immunology*, 20, 389–391, <https://doi.org/10.1038/s41577-020-0343-0>.
- Trautz, B., Wiedemann, H., Lüchtenborg, C., Pierini, V., Kranich, J., Glass, B., Kräusslich, H.-G., Brocker, T., Pizzato, M., Ruggieri, A., Brügger, B., & Fackler, O. T. (2017). The host-cell restriction factor SERINC5 restricts HIV-1 infectivity without altering the lipid composition and organization of viral particles. *Journal of Biological Chemistry*, 292(33), 13702–13713, <http://doi.org/10.1074/jbc.m117.797332>.
- van der Zee, P. M., Biró, E., Ko, Y., de Winter, R. J., Hack, C. E., Sturk, A., & Nieuwland, R. (2006). P-selectin- and CD63-exposing platelet microparticles reflect platelet activation in peripheral arterial disease and myocardial infarction. *Clinical Chemistry*, 52, 657–664, <https://doi.org/10.1373/clinchem.2005.057414>.
- Wang, R. H., Phillips, G. Jr., Medof, M. E., & Mold, C. (1993). Activation of the alternative complement pathway by exposure of phosphatidylethanolamine and phosphatidylserine on erythrocytes from sickle cell disease patients. *Journal of Clinical Investigation*, 92, 1326–1335, <https://doi.org/10.1172/JCI116706>.
- Wölfel, R., Corman, V. M., Guggemos, W., Seilmaier, M., Zange, S., Müller, M. A., Niemeyer, D., Jones, T. C., Vollmar, P., Rothe, C., Hoelscher, M., Bleicker, T., Brünink, S., Schneider, J., Ehmann, R., Zwirgmaier, K., Drosten, C., & Wendtner, C. (2020). Virological assessment of hospitalized patients with COVID-2019. *Nature*, 581, 465–469, <https://doi.org/10.1038/s41586-020-2196-x>.
- WorldHealthOrganization (2020). Novel Coronavirus: COVID-19 Therapeutic Trial Synopsis. WHO R&D Blueprint, Draft February 18, 2020. www.who.int/blueprint/priority-diseases/key-action/COVID-19_Treatment_Trial_Design_Master_Protocol_synopsis_Final_18022020.pdf
- Yang, X., Yu, Y., Xu, J., Shu, H., Xia, J., Liu, H., Wu, Y., Zhang, L., Yu, Z., Fang, M., Yu, T., Wang, Y., Pan, S., Zou, X., Yuan, S., & Shang, Y. (2020). Clinical course and outcomes of critically ill patients with SARS-CoV-2 pneumonia in Wuhan, China: A single-centered, retrospective, observational study. *The Lancet Respiratory Medicine*, 8, 475–481, [https://doi.org/10.1016/S2213-2600\(20\)30079-5](https://doi.org/10.1016/S2213-2600(20)30079-5).
- Zaid, Y., Puhm, F., Allaey, I., Naya, A., Oudghiri, M., Khalki, L., Limami, Y., Zaid, N., Sadki, K., Ben El Haj, R., Mahir, W., Belayachi, L., Belefquih, B., Benouda, A., Cheikh, A., Langlois, M. A., Cherrah, Y., Flamand, L., Guessous, F., & Boilard, E. (2020). Platelets can associate with SARS-Cov-2 RNA and are hyperactivated in COVID-19. *Circulation Research*, 127, 1404–18, <https://doi.org/10.1161/CIRCRESAHA.120.317703>.
- Zhang, Y., Xiao, M., Zhang, S., Xia, P., Cao, W., Jiang, W., Chen, H., Ding, X., Zhao, H., Zhang, H., Wang, C., Zhao, J., Sun, X., Tian, R., Wu, W., Wu, D., Ma, J., Chen, Y., Zhang, D., ... Zhang, S. (2020). Coagulopathy and antiphospholipid antibodies in patients with Covid-19. *The New England Journal of Medicine*, 382, e38, <https://doi.org/10.1056/NEJMc2007575>.
- Zheng, H. Y., Zhang, M., Yang, C. X., Zhang, N., Wang, X. C., Yang, X. P., Dong, X. Q., & Zheng, Y. T. (2020). Elevated exhaustion levels and reduced functional diversity of T cells in peripheral blood may predict severe progression in COVID-19 patients. *Cellular & Molecular Immunology*, 17, 541–543, <https://doi.org/10.1038/s41423-020-0401-3>.
- Zheng, M., Gao, Y., Wang, G., Song, G., Liu, S., Sun, D., Xu, Y., & Tian, Z. (2020). Functional exhaustion of antiviral lymphocytes in COVID-19 patients. *Cellular & Molecular Immunology*, 17, 533–535, <https://doi.org/10.1038/s41423-020-0402-2>.
- Zhou, R., To, K. K., Wong, Y. C., Liu, L., Zhou, B., Li, X., Huang, H., Mo, Y., Luk, T. Y., Lau, T. T., Yeung, P., Chan, W. M., Wu, A. K., Lung, K. C., Tsang, O. T., Leung, W. S., Hung, I. F., Yuen, K. Y., & Chen, Z. (2020). Acute SARS-CoV-2 infection impairs dendritic cell and T cell responses. *Immunity*, 53, 864–877 e865, <https://doi.org/10.1016/j.immuni.2020.07.026>.

SUPPORTING INFORMATION

Additional supporting information may be found in the online version of the article at the publisher's website.

How to cite this article: Rausch, L., Lutz, K., Schifferer, M., Winheim, E., Gruber, R., Oesterhaus, E. F., Rinke, L., Hellmuth, J. C., Scherer, C., Muenchhoff, M., Mandel, C., Bergwelt-Baildon, M., Simons, M., Straub, T., Krug, A. B., Kranich, J., & Brocker, T. (2021). Binding of phosphatidylserine-positive microparticles by PBMCs classifies disease severity in COVID-19 patients. *Journal of Extracellular Vesicles*, 10, e12173. <https://doi.org/10.1002/jev2.12173>